Catalysis Letters
https://doi.org/10.1007/s10562-019-02986-2

New Copper Complex on Fe_3O_4 Nanoparticles as a Highly Efficient Reusable Nanocatalyst for Synthesis of Polyhydroquinolines in Water

Muhammad Aqeel Ashraf[1,2] · **Zhenling Liu**[3] · **Wan-Xi Peng**[1] · **Caixia Gao**[4]

Received: 21 August 2019 / Accepted: 27 September 2019

Abstract

In this work, we present a simple, environmentally friendly and economical route for the preparation of a novel copper-Schiff-base organometallic complex on Fe_3O_4 nanoparticles (Fe_3O_4@Schiff-base-Cu) using an inexpensive and simple method and available materials. This magnetic nanocatalyst was comprehensively characterized using Fourier transform infrared spectroscopy (FT-IR), X-Ray Diffractometer (XRD), inductively coupled plasma atomic emission spectroscopy (ICP), energy-dispersive X-ray spectroscopy (EDS), scanning electron microscopy (SEM), X-ray mapping, thermogravimetric analysis (TGA) and vibrating sample magnetometer (VSM) analysis. In the second stage, the catalytic activity of this catalyst was studied in the synthesis of polyhydroquinoline derivatives via Hantzsch reaction in water as a green solvent. In this sense, simple preparation of the catalyst from the commercially available materials, high catalytic activity, simple operation, short reaction times, high yields and use of green solvent can be regarded as some advantages of this protocol. In addition, it is worth mentioning that this nanocatalyst was easily recovered using external magnet and reused for several times without significant loss of its catalytic efficiency. Finally, the leaching, heterogeneity and stability of Fe_3O_4@Schiff-base-Cu were studied by hot filtration test and ICP technique.

Graphic Abstract

A green and novel Fe_3O_4@Schiff-base-Cu catalyst sucssesfully was prepared and characterized. This catalyst can be used for the Synthesis of polyhydroquinolines in water as the green solvent. This catalyst could be recovered easily and reused many times without important decrease in efficiency.

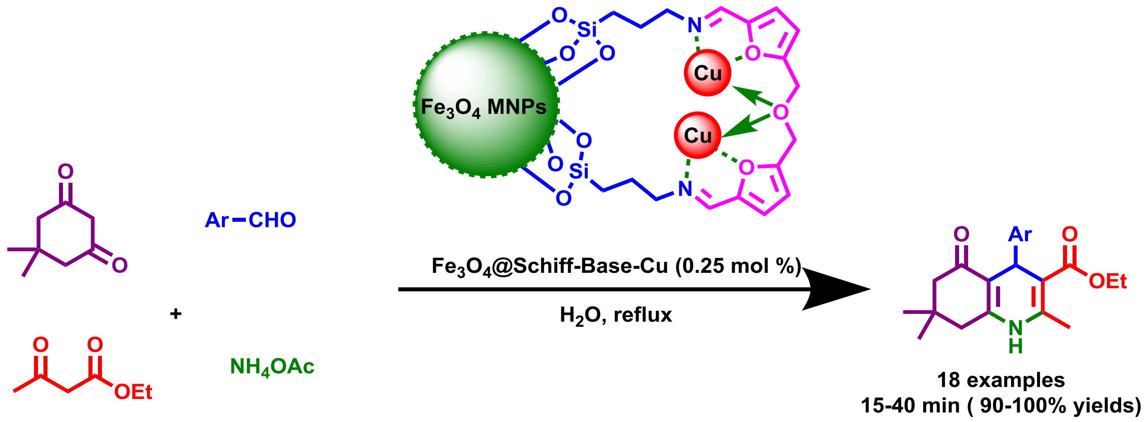

Keywords Fe_3O_4@Schiff-base-Cu · Polyhydroquinolines · Hantzsch reaction · Reusable catalyst

---

✉ Wan-Xi Peng
pengwanxi163@gmail.com; pengwanxi@163.com

Extended author information available on the last page of the article

1 Introduction

polyhydroquinoline derivatives have a wide range of biological activities such as bronchodilator, antiatherosclerotic, antitumor and antidiabetic and vasodilator properties [1–6] i.e. polyhydroquinoline derivatives which can be considered as a significant class of the well-known Ca^{2+} channel blockers establish the skeletons of drug molecules utilized in the treatment of hypertension and cardiovascular diseases [7, 8]. Therefore, the synthesis of polyhydroquinoline derivatives can be viewed as an area of remarkable attention in organic chemistry. The use of copper catalysts for this transformation is still interesting from an industrial perspective because of the fact that copper is less toxic and inexpensive than other transition metals [9–16]. Homogenous Cu complexes which are among the most representative Cu catalysts are coordinated with different organic ligands and provide excellent yields [17–21]. However, the homogenous Cu complexes suffer from significant drawbacks; including, the difficulty of separation and recovery of Cu complexes from the reaction system, high costs and the potential environmental pollution [20, 22–24]. In order to circumvent these issues and regarding the rapid advancement of nanotechnology, heterogeneous copper catalysts have been proposed by supporting Cu nanoparticles on the surface of the insoluble hosts [25–29]. Recently, the nanomaterials have widely attracted much attention due to the fact that they are applied as a precursor of inorganic–organic hybrid materials [24, 30–35]. Moreover, they have excellent applications in catalytic reactions, adsorption materials, optical and environmental problems, food processing, medical industry, energy production and they have also been used in various fields of chemistry, physics, engineering and science [36–41]. Besides, magnetic Fe_3O_4 nanoparticle has attracted great attention due to its intrinsic magnetic property, facile synthesis and being environment-friendly with high surface area, low cost and good chemical stability [42–45]. Among the various methods for the synthesis of Fe_3O_4 MNPs, the coprecipitation method has several advantages such as production in a one-pot process, green conditions, and low time of synthesis [46–49]. The Schiff bases are essential class of organic ligands, and their metal complexes have been extensively exploited in a wide variety of organic reactions especially in the multicomponent reactions [50, 51]. In this sense, they can become possible alternatives to other ligands [41] owing to the advantages such as their cost-effectiveness, availability, ease of synthesis, and chemical and thermal stability [50–56]. Researchers have developed these ligands and their metal complexes, which afforded more effective and easier oxidative addition. Schiff bases are common ligands in coordination chemistry, due to their unique properties of forming stable complexes [57, 58]. During the last two decades, schiff base ligands have been leading the world of catalysis in an unprecedented manner [59–62]. Schiff base-transition metal complexes have been extensively used as catalysts for various organic reactions such as cross- coupling reactions, multicomponent reactions, degradations, substitution reaction, elimination reaction, addition reaction, radical reactions and oxidation–reduction reactions [50, 55, 63–70]. Thus, for the researchers, schiff base ligands have become of vital interest to understand the fundamental reasons behind their catalytic behavior [71–78]. Rational catalysts design, by proper functionalization of schiff base ligands to explore their utility in a host of catalytically relevant syntheses of interest to contemporary organic transformations, is thus central to industrial and academic research [77, 79]. Various synthetic methodologies have been developed using heterogenized organometallic schiff base catalysis [80–91]. However, in this report, copper complex supported on surface-modified Fe_3O_4 nanoparticles (Fe_3O_4@Schiff-base-Cu) is introduced as a new and efficient reusable catalyst for the synthesis of polyhydroquinoline derivatives.

The results of this study differ from the previously reported literatures due to the less number of catalyst synthesis steps. Also, the final complex can be synthesized using a stable interaction between the amine and ether groups of the prepared Schiff base ligand and the Cu atom. In addition, the presence of both of these electron-donor functional groups in the prepared Schiff base structure, which can form a stable complex with Cu, can also reduce the leaching of Cu into the reaction media. Moreover, water was used as a green solvent under aerobic reaction conditions. Besides, the catalyst could be easily separated by applying a simple magnet and could also be reused in several consecutive runs without appreciable change in its catalytic activity. Noteworthy, features of this catalyst are high conversion yields (less reactive substrates) and good selectivity.

2 Experimental

2.1 Preparation of Fe_3O_4@Schiff-Base-Cu Catalyst

The Fe_3O_4 magnetic nanoparticles were prepared by the coprecipitation technique as it was previously reported [92]. For the synthesis of the supported Fe_3O_4@Schiff-Base-Cu complex, 1 g of the prepared Fe_3O_4 nanoparticles was dispersed in 50 mL ethanol/water (1:1) by sonication for 15 min. and, then, 1.5 mL 3-aminopropyltrimethoxysilane (APTMS) was added to the reaction mixture. The reaction mixture was stirred under the N_2 atmosphere at 40 °C for 24 h. Then, the obtained Fe_3O_4@APTMS MNPs product was separated by magnetic decantation, washed with ethanol and, then, dried at 90 °C in an oven for 4 h. Afterwards, the Schiff-Base ligand supported on heterogeneous Fe_3O_4 was obtained by the reaction of O-bisMe-furaldehyde (5,5′-Oxybis(5-methylene-2-furaldehyde)) (2.5 mmol) with the amine groups on the surface of Fe_3O_4@APTMS (1 g) in ethanol (20 mL) overnight and under nitrogen atmosphere and reflux conditions. The target Fe_3O_4@Schiff-base was obtained by magnetic separation, washed with ethanol, and dried at 80 °C in an oven for 4 h. Finally, In order to prepare Fe_3O_4@Schiff-Base-Cu organometallic complex, the obtained Fe_3O_4@Schiff-base (0.1 g) was dispersed in 30 mL ethanol by sonication for 30 min and, then, $Cu(NO_3)_2 \cdot 3H_2O$ (0.5 g) was added to the reaction mixture. The reaction mixture was stirred at 80 °C for 24 h. Then, the final product (Fe_3O_4@Schiff-Base-Cu) was separated using an external magnet, washed with water and ethanol and dried at 80 °C in an oven for 4 h.

2.2 General Procedure for the Synthesis of Polyhydroquinolines

A mixture of aldehyde (1 mmol), dimedon (1 mmol), ethylacetoacetate (1 mmol) and ammonium acetate (1.3 mmol) was dissolved in 3 mL water in the presence of Fe_3O_4@ Schiff-Base-Cu catalyst (0.25 mol% of Cu) and stirred at reflux conditions. The progress of the reaction was monitored by TLC. After the completion of the reaction, the catalyst was separated by a magnet and washed with ethanol. Then, the solvent was evaporated and, finally, all the products were recrystallized in ethanol.

2.3 Selected Spectral Data

2.3.1 Ethyl 4-(4-chlorophenyl)-2,7,7-trimethyl-5-oxo-1,4,5,6,7,8-hexahydroquinoline-3-carboxylate (Table 2 Entry 1)

^{1}H NMR (400 MHz, DMSO-d6) δ = 9.12 (s, 1H, NH) 7.25 (d, J = 8.0 Hz, 2H), 7.16 (d, J = 8.4 Hz, 2H), 4.83 (s, 1H), 3.99 (q, J = 7.2 Hz, 2H), 2.43 (d, J = 17.2 Hz, 1H), 2.25–2.28 (m, 4H), 2.19 (d, J = 16.0 Hz, 1H), 1.99 (d, J = 16.0 Hz, 1H), 1.13 (t, J = 7.2 Hz, 3H), 1.00 (s, 3H), 0.83 (s, 3H). ^{13}C NMR (50 MHz, DMSO-d6) δ = 194.1, 166.5, 149.5, 146.5, 145.3, 130.2, 129.2, 127.6, 109.6, 103.0, 59.0, 50.1, 35.6, 32.1, 29.0, 26.4, 18.3, 4.1.

2.3.2 Ethyl 4-(4-methoxyphenyl)-2,7,7-trimethyl-5-oxo-1,4,5,6,7,8-hexahydroquinoline-3-carboxylate (Table 2 Entry 3)

^{1}H NMR (400 MHz, DMSO-d6) δ = 9.00 (s, 1H, NH), 7.05 (d, J = 8.4 Hz, 2H), 6.74 (d, J = 8.4 Hz, 2H), 4.78 (s, 1H), 3.99 (q, J = 7.2 Hz, 2H), 3.67 (s, 3H, OCH_3), 2.43 (d, J = 16.8 Hz, 1H), 2.29 (m, 4H), 2.17 (d, J = 16.0 Hz, 1H), 1.98 (d, J = 16.0 Hz, 1H), 1.15 (t, J = 7.2 Hz, 3H), 1.00 (s, 3H), 0.85 (s, 3H). ^{13}C NMR (100 MHz, DMSO-d_6) δ = 194.2, 166.9, 157.3, 149.2, 144.6, 140.0, 128.4, 113.1, 110.1, 103.9, 59.0, 54.8, 50.3, 34.9, 32.1, 29.1, 26.5, 18.2, 14.2.

2.3.3 Ethyl 4-(3,4-dimethoxyphenyl)-2,7,7-trimethyl-5-oxo-1,4,5,6,7,8-hexahydroquinoline-3-carboxylate (Table 2 Entry 4)

^{1}H NMR (400 MHz, DMSO-d6) δ = 9.02 (s, 1H, NH), 6.77–6.74 (m, 2H), 6.63 (dd, J = 2.0 & 8.4 Hz 1H), 4.79 (s, 1H), 4.02 (q, J = 7.2 Hz, 2H), 3.66 (s, 3H, OCH_3), 3.65 (s, 3H, OCH_3), 2.44 (d, J = 17.2 Hz, 1H), 2.30–2.26 (m, 4H), 2.19 (d, J = 16.4 Hz, 1H), 2.00 (d, J = 16.4 Hz, 1H), 1.17 (t, J = 7.2 Hz, 3H), 1.01 (s, 3H), 0.88 (s, 3H). ^{13}C NMR (50 MHz, DMSO-d6) δ = 194.2, 166.8, 149.3, 147.9, 146.9, 144.5, 140.4, 119.2, 111.7, 111.4, 110.0, 103.8, 59.0, 55.4, 55.3, 50.3, 35.1, 32.1, 29.2, 26.4, 18.2, 14.2.

2.3.4 Ethyl 2,7,7-trimethyl-5-oxo-4-(4-(trifluoromethyl)phenyl)-1,4,5,6,7,8-hexahydroquinoline-3-carboxylate (Table 2 Entry 5)

^{1}H NMR (400 MHz, DMSO-d_6) δ = 9.17 (s, 1H, NH), 7.57 (d, J = 7.6 Hz, 2H), 7.37 (d, J = 8.0 Hz, 2H), 4.93 (s, 1H), 3.99 (q, J = 7.2 Hz, 2H), 2.45 (d, J = 16.4 Hz, 1H), 2.32 (m, 4H), 2.19 (d, J = 16.4 Hz, 1H), 2.00 (d, J = 16.0 Hz, 1H), 1.13 (t, J = 7.2 Hz, 3H), 1.00 (s, 3H), 0.83 (s, 3H). ^{13}C NMR (50 MHz, DMSO-d_6) δ = 194.1, 166.6, 151.8, 149.8, 145.7, 128.2, 124.7, 124.6, 109.3, 102.8, 59.1, 50.1, 36.3, 32.1, 29.0, 26.5, 18.3, 14.1.

2.3.5 Ethyl 4-(4-cyanophenyl)-2,7,7-trimethyl-5-oxo-1,4,5,6,7,8-hexahydroquinoline-3-carboxylate (Table 2 Entry 6)

^{1}H NMR (400 MHz, DMSO-d6) δ = 9.19 (s, 1H, NH), 7.68 (d, J = 8.0 Hz, 2H), 7.34 (d, J = 8.0 Hz, 2H), 4.90 (s, 1H), 3.98 (q, J = 7.2 Hz, 2H), 2.44 (d, J = 17.2 Hz, 1H), 2.30–2.26 (m, 4H), 2.19 (d, J = 16.4 Hz, 1H), 1.99 (d, J = 16.4 Hz, 1H), 1.12 (t, J = 7.2 Hz, 3H), 1.00 (s, 3H), 0.81 (s, 3H).^{13}C NMR (50 MHz, DMSO-d6) δ = 194.1, 166.3, 152.8, 149.9, 146.0, 131.8, 128.5, 119.0, 109.1, 108.5, 102.4, 59.1, 50.1, 36.7, 32.1, 29.0, 26.4, 18.3, 14.1.

2.3.6 Ethyl 4-(3,4-dihydroxyphenyl)-2,7,7-trimethyl-5-oxo-1,4,5,6,7,8-hexahydroquinoline-3-carboxylate (Table 2 Entry 10)

^{1}H NMR (400 MHz, DMSO-d_6) δ = 8.94 (s, 1H, NH), 8.56 (s, 1H, OH), 8.45 (s, 1H, OH), 6.57 (d, J = 2.0 Hz, 1H), 6.51

(d, J = 8.0 Hz, 1H), 6.39 (dd, J = 2.0 and 8.4 Hz, 1H), 4.68 (s, 1H), 4.00 (q, J = 7.2 Hz, 2H), 2.40 (d, J = 17.2 Hz, 1H), 2.27 (m, 4H), 2.16 (d, J = 16.0 Hz, 1H), 1.99 (d, J = 16.0 Hz, 1H), 1.16 (t, J = 7.2 Hz, 3H), 1.00 (s, 3H), 0.87 (s, 3H). ^{13}C NMR (100 MHz, DMSO-d_6) δ = 194.3, 167.1, 149.0, 144.6, 144.1, 143.1, 138.6, 118.1, 115.2, 114.8, 110.3, 104.1, 59.0, 50.4, 34.9, 32.1, 29.2, 26.6, 18.0, 14.2.

2.3.7 Ethyl 2,7,7-trimethyl-4-(4-nitrophenyl)-5-oxo-1,4,5,6,7,8-hexahydroquinoline-3-carboxylate (Table 2 Entry 14)

^1H NMR (400 MHz, DMSO-d_6) δ = 9.23 (s, 1H, NH), 8.10 (d, J = 8.8 Hz, 2H), 7.42 (d, J = 8.8 Hz, 2H), 4.96 (s, 1H), 3.98 (q, J = 7.2 Hz, 2H), 2.45 (d, J = 16.4 Hz, 1H), 2.27–2.31 (m, 4H), 2.20 (d, J = 16.0 Hz, 1H), 1.99 (d, J = 16.0 Hz, 1H), 1.12 (t, J = 7.2 Hz, 3H), 1.00 (s, 3H), 0.82 (s, 3H), ^{13}C NMR (50 MHz, DMSO-d6) δ = 194.1, 166.3, 154.9, 150.0, 146.0, 145.6, 128.7, 123.0, 109.0, 102.3, 59.2, 50.0, 36.6, 32.1, 29.0, 26.4, 18.3, 14.0.

2.3.8 Ethyl 2,7,7-trimethyl-4-(3-nitrophenyl)-5-oxo-1,4,5,6,7,8-hexahydroquinoline-3-carboxylate (Table 2 Entry 15)

^1H NMR (400 MHz, DMSO-d_6) δ = 9.24 (s, 1H, NH), 7.98 (m, 2H), 7.62–7.50 (m, 2H), 4.96 (s, 1H), 3.98 (q, J = 7.2 Hz, 2H), 2.48 (d, J = 17.2 Hz, 1H), 2.38 (m, 4H), 2.21 (d, J = 16.0 Hz, 1H), 2.00 (d, J = 16.4 Hz, 1H), 1.13 (t, J = 7.2 Hz, 3H), 1.01 (s, 3H), 0.83 (s, 3H). ^{13}C NMR (50 MHz, DMSO-d6) δ = 194.2, 166.3, 150.3, 149.6, 147.3, 146.0, 134.2, 129.3, 121.9, 120.8, 109.2, 102.6, 59.2, 50.0, 36.4, 32.2, 29.0, 26.3, 18.3, 14.0,

2.3.9 Ethyl 4-(5-hydroxy-2-nitrophenyl)-2,7,7-trimethyl-5-oxo-1,4,5,6,7,8-hexahydroquinoline -3-carboxylate (Table 2 Entry 16)

^1H NMR (400 MHz, DMSO-d_6) δ = 10.37 (s, 1H, OH), 9.06 (s, 1H, NH), 7.69 (d, J = 8.8 Hz, 1H), 6.75 (d, J = 2.4 Hz, 1H), 6.62 (dd, J = 2.4 & 8.8 Hz, 1H), 5.77 (s, 1H), 3.94 (q, J = 7.2 Hz, 2H), 2.42 (d, J = 16.8 Hz, 1H), 2.29 (s, 3H), 2.25 (d, J = 16.8 Hz, 1H), 2.13 (d, J = 15.6 Hz, 1H), 1.92 (d, J = 15.6 Hz, 1H), 1.00 (t, J = 7.2 Hz, 3H), 0.98 (s, 3H), 0.79 (s, 3H). ^{13}C NMR (100 MHz, DMSO-d6) δ = 193.9, 166.7, 161.5, 149.4, 145.8, 145.4, 140.1, 126.3, 166.5, 113.3, 100.3, 103.5, 59.0, 50.1, 32.0, 31.7, 28.8, 26.3, 18.2, 13.8.

3 Results and Discussion

3.1 Catalyst Preparation

The presented work tries to describe a novel Cu-Schiff-base immobilized on Fe_3O_4 as a reusable magnetic nanocatalyst. Initially, the modified Fe_3O_4 nanoparticles with 3-aminoropropyltriethoxysilane (Fe_3O_4@APTMS MNPs) have been prepared according to the reported procedure [93]. Then, the

Scheme 1 Stepwise preparation of Fe_3O_4@Schiff-Base-Cu

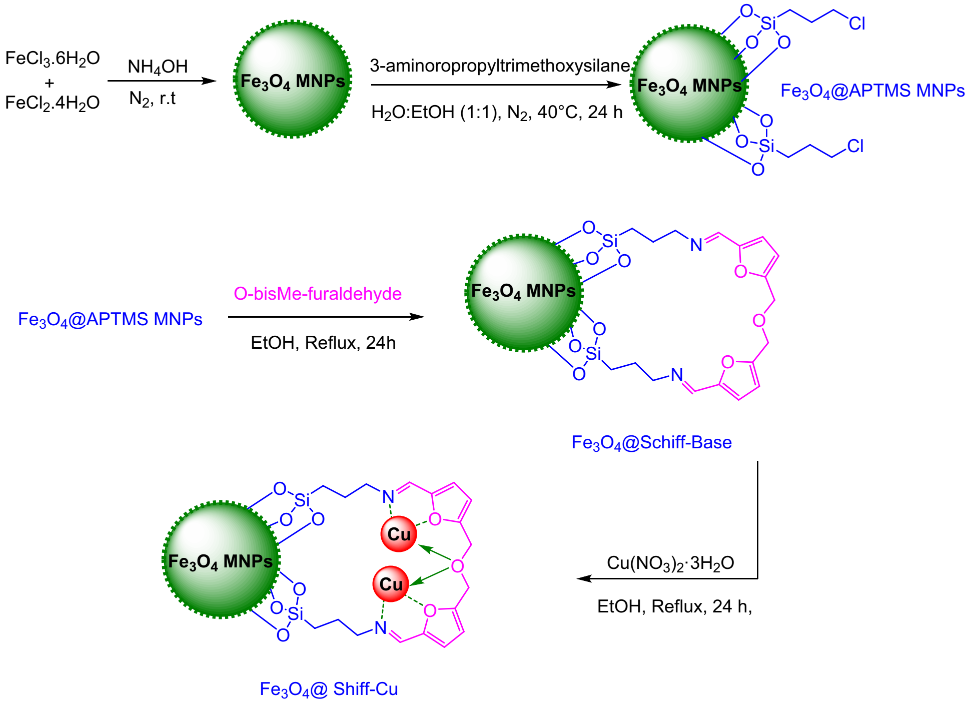

Schiff-base ligand was synthesized via the substitution reaction of NH_2 with O-bisMe-furaldehyde. Finally, the catalyst was synthesized by the reaction of Fe_3O_4@Schiff-Base with $Cu(NO_3)_2 \cdot 3H_2O$ (Scheme 1). This catalyst has been characterized by FT-IR, XRD, EDS, ICP, SEM, X-ray mapping TGA and VSM techniques.

3.2 Catalyst Characterizations

The as-prepared Fe_3O_4@Schiff-base-Cu catalyst was also characterized by FT-IR, XRD, EDS, VSM, ICP, TGA, SEM, and X-ray mapping techniques.

The FT-IR spectra for the Fe_3O_4 MNPs (a), Fe_3O_4 @ AMPTMS MNPs (b), Fe_3O_4@Schiff-Base (c) and Fe_3O_4@ Schiff-base-Cu (d) are shown in Fig. 1. The strong absorption at 590 and 628 cm^{-1} in spectrums was attributed to the presence of Fe–O stretching vibration [94]. In addition, the peak appearing at 1624 cm^{-1} was attributed to the bending vibration of OH band or the stretching vibrational mode of the adsorbed water layer [95]. Moreover, the broad band at around 3392 cm^{-1} is attributed to the asymmetric and symmetric stretching vibrations of –OH band of the Fe_3O_4 nanoparticles surface [96]. In the curve of Fe_3O_4@APTMS MNPs (b), two peaks at 2853 and 2925 cm^{-1} can be attributed to the C–H stretching vibrations of NH_2-propyl group [93, 97, 98]. Besides, the peak at 892 cm^{-1} can be attributed to the Fe–O–Si stretching vibration. Moreover, a strong IR peak which appeared at 1648 cm – 1 corresponded to the strong bending vibration of the amide I group and showed the successful immobilization of the anchored NH_2-propyl group on the Fe_3O_4 Support [93, 97]. Absorption peaks at 1012 and 1560 cm^{-1} (C–N stretching vibration) in Fe_3O_4@Schiff-base provide evidences confirming the formation of the desired ligand [66, 99, 100]. The shift on the absorption peak at approximately 1624 cm^{-1} (C=N stretching vibration) in the Fe_3O_4@Schiff-base-Cu spectra is due to the complexion of Cu ions with Fe_3O_4@Schiff-base [101].

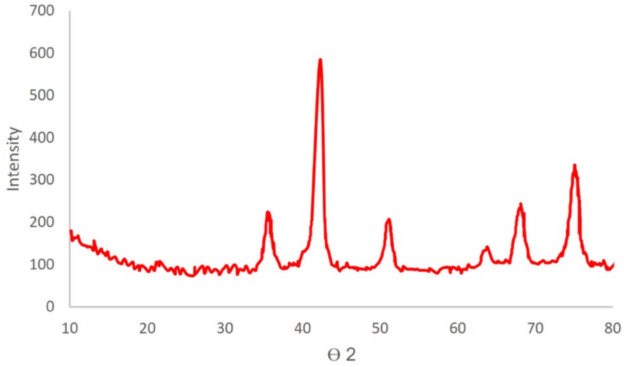

Fig. 2 XRD pattern of the Fe_3O_4@Schiff-Base-Cu

The X-ray diffraction analysis (XRD) pattern of Fe_3O_4@ Schiff-base-Cu is shown in Fig. 2, in which the peak positions of 2θ at 35.27, 41.52, 50.56, 63.24, 67.49, 74.47, correspond to the (2 2 0), (3 1 1), (4 0 0), (4 2 2), (5 1 1), and (4 4 0) reflections, respectively, as they are in agreement with the standard XRD pattern of Fe_3O_4 nanoparticles [102]. More importantly, the phase of Fe_3O_4 support is not destroyed during the immobilization of Schiff-base-Cu organometallic complex on iron oxide layers. In addition, the Crystalline size of Fe_3O_4@Schiff-Base-Cu MNPs was estimated, using the Scherrer equation from XRD pattern data, to be 20.15 ± 1 nm.

The elemental composition of the Fe_3O_4@Schiff-base-Cu organometallic complex was determined using EDX analysis (Fig. 3). The presence of Fe, O, Si, C, N, and Cu in EDX pattern provides evidences confirming the formation of the organometallic complex. In addition, the exact amount of

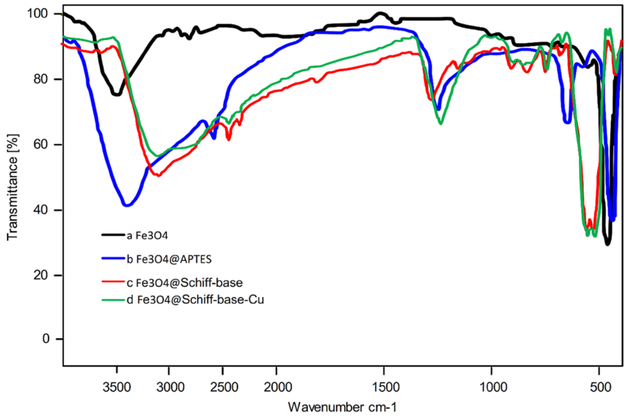

Fig. 1 FT-IR spectra for the Fe_3O_4 MNPs (a), Fe_3O_4 @APTMS MNPs (b), Fe_3O_4@Schiff-Base (c) and Fe_3O_4@Schiff-base-Cu (d)

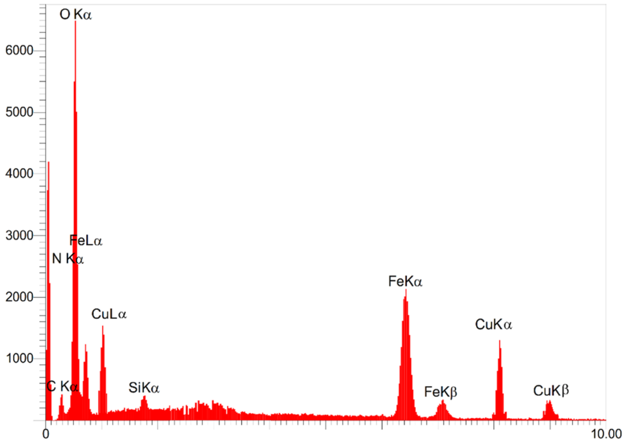

Fig. 3 EDS spectrum of the Fe_3O_4@Schiff-Base-Cu

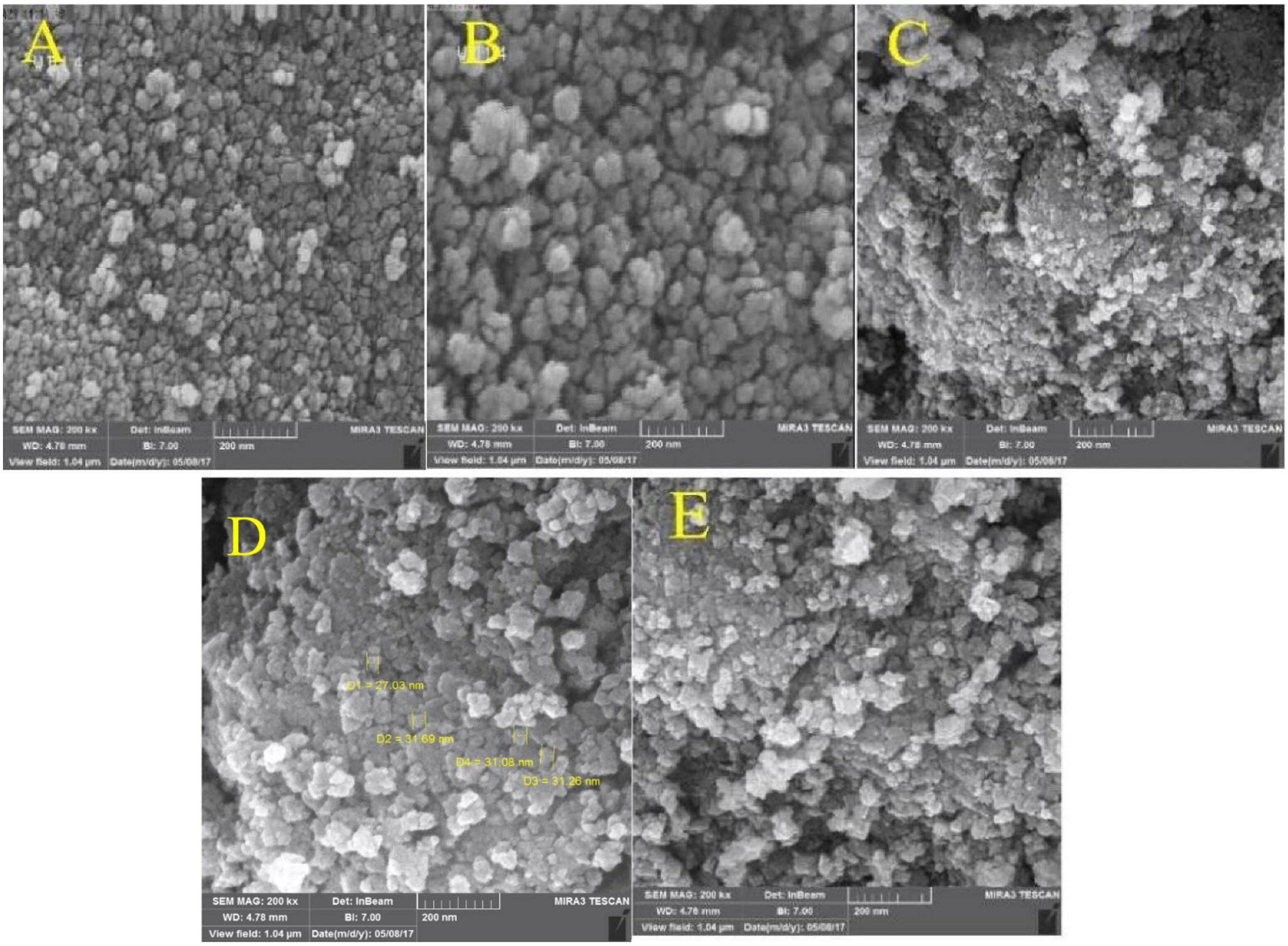

Fig. 4 SEM images of the Fe_3O_4 MNPs (**a**), Fe_3O_4@APTMS MNPs (**b**), Fe_3O_4@Schiff-Base (**c**) and Fe_3O_4@Schiff-base-Cu (**d**) and recovers Fe_3O_4@Schiff-base-Cu complex (**e**)

Cu, which was immobilized on Fe_3O_4@Schiff-base, was obtained by ICP-OSE as 0.92×10^{-3} mol g^{-1}.

Figure 4 illustrates the morphology of Fe_3O_4 MNPs (a), Fe_3O_4 @APTMS MNPs (b) Fe_3O_4@Schiff-base (c) and Fe_3O_4@Schiff-base-Cu complex (d), and recovers Fe_3O_4@Schiff-base-Cu complex (e) as probed by the scanning electron microscopy (SEM) technique. As shown in Fig. 4, the SEM image of Fe_3O_4@Schiff-Base-Cu complex shows spherical morphology for most particles.

The size and morphology of Fe_3O_4@Schiff-base-Cu complex were investigated using TEM. As shown in Fig. 5, the magnetic cores of the nanoparticles were uniform in both size and shape. Moreover, the particle size was measured to be about 15–25 nm and, consequently, the spherical morphology was confirmed. The results of TEM is in agreement with SEM and XRD results.

The X-ray mapping of Fe_3O_4@Schiff-base-Cu nanocatalyst is shown in Fig. 6. The good dispersion of Cu on the surface of the catalyst was confirmed using the elemental map images.

Figure 7 illustrates the TGA diagram of Fe_3O_4@Schiff-base-Cu complex. The small weight loss between 5% below 200 °C was exhibited and attributed to the evaporation of the physically adsorbed solvents and surface hydroxyl groups [94]. Besides, the next weight loss about 15% occurred between 200 and 600 °C which are related to the decomposition of the functional groups chemisorbed onto the surface of the catalyst support [103]. The obtained results confirmed the formation of the desired organometallic complex on the Fe_3O_4 Support.

Magnetic measurement of the catalyst was analysed by a vibrating sample magnetometer (VSM) at room temperature. Figure 8 exhibits the magnetization curves of Fe_3O_4 and Fe_3O_4@Schiff-Base-Cu. The value of the saturation magnetic moment of the Fe_3O_4@Schiff-base-Cu complex (Blue diagram) is 51.3 emu/g as compared to the saturation magnetization of Fe_3O_4 which was found to be 78 emu/g. This decrease in the saturation magnetization of Fe_3O_4@Schiff-Base-Cu complex is due to the successful grafting of

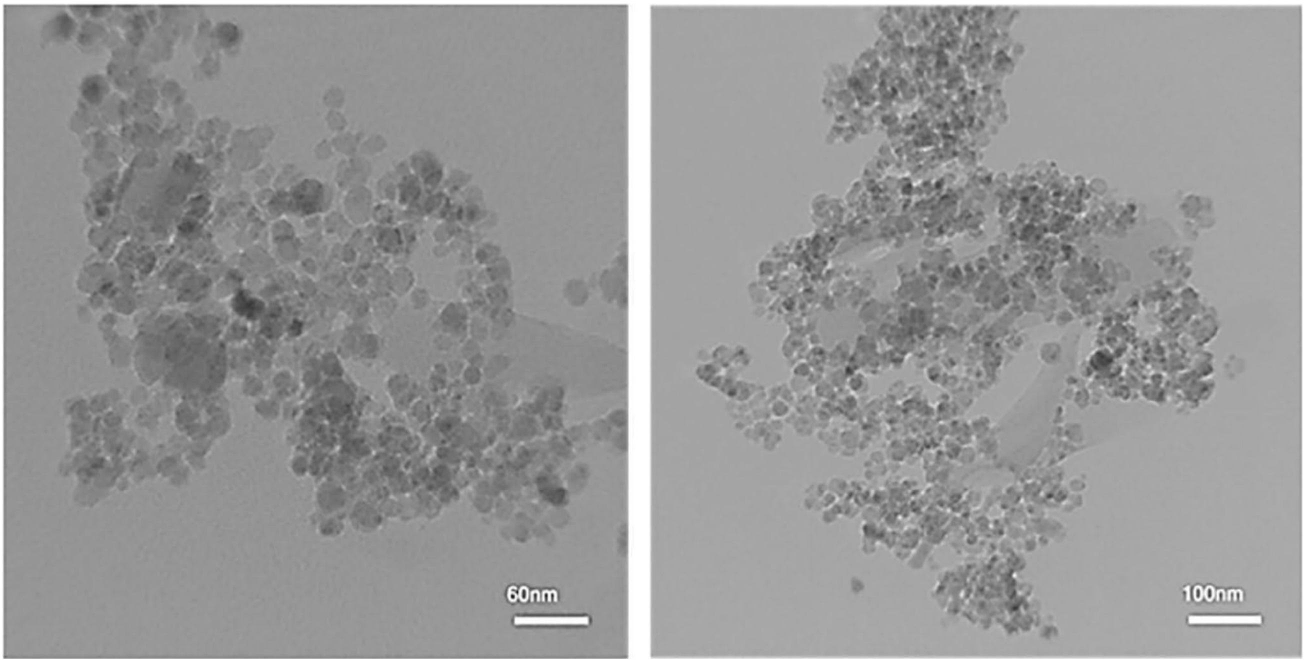

Fig. 5 TEM images of Fe_3O_4@Schiff-base-Cu nanocatalyst

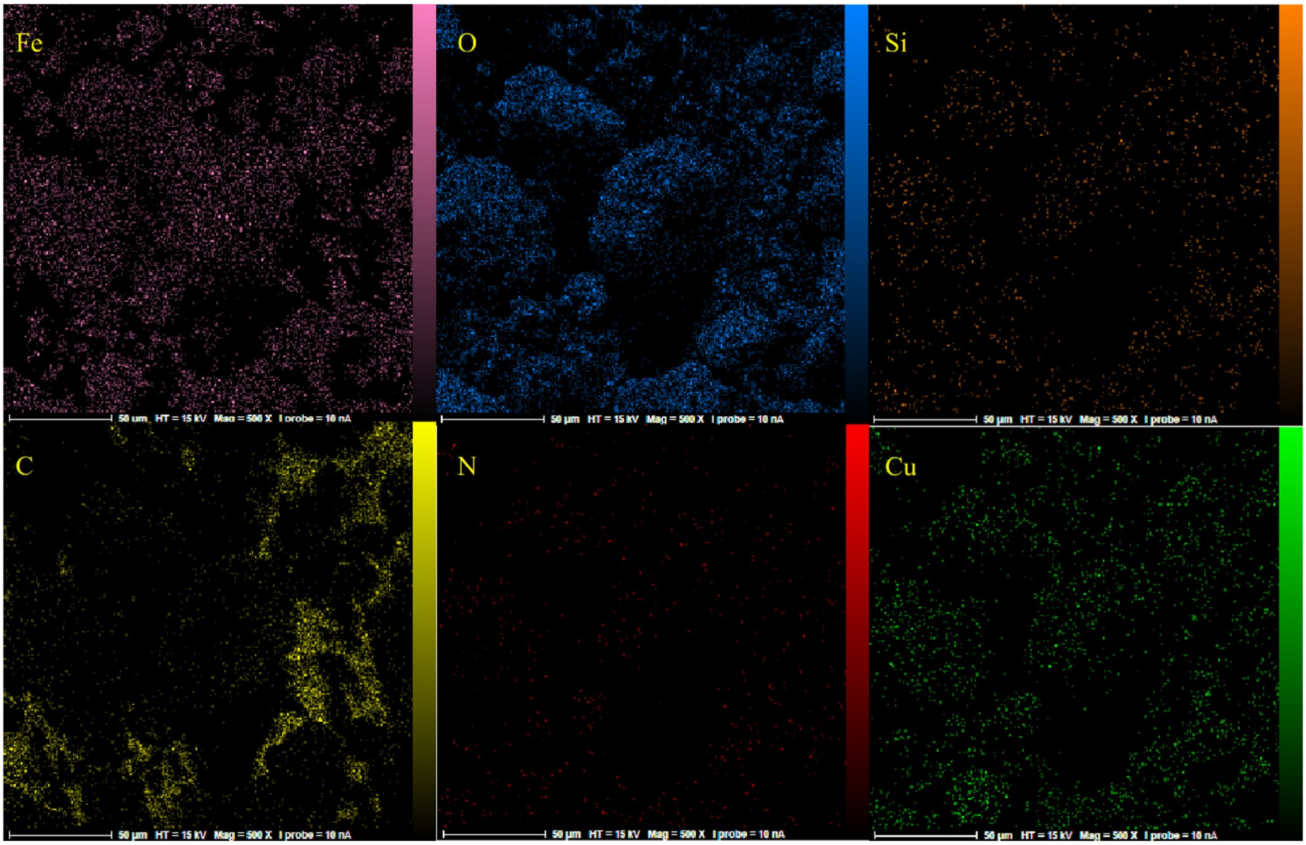

Fig. 6 X-ray mapping images of the Fe_3O_4@Schiff-Base-Cu

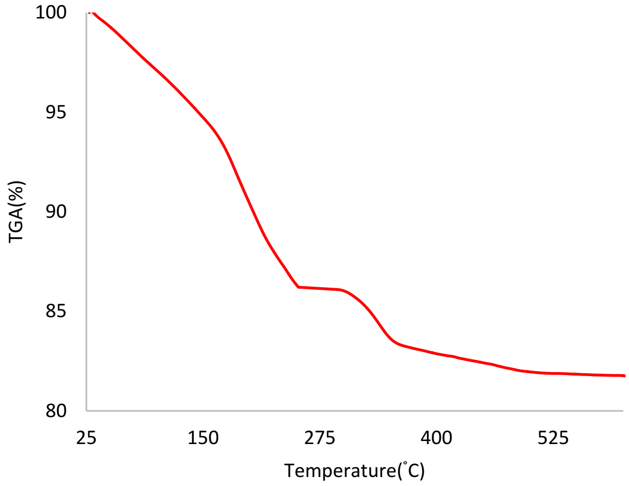

Fig. 7 TGA diagram of Fe_3O_4@Schiff-base-Cu complex

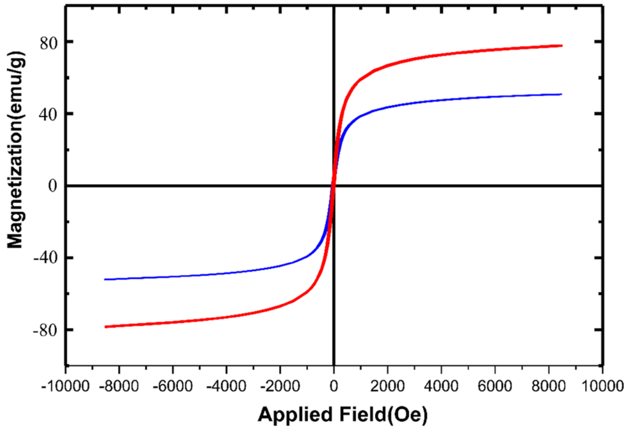

Fig. 8 VSM spectrum of Fe_3O_4(Red) and @Schiff-Base-Cu (Blue)

Schiff-Base-Cu complex on the surface of Fe_3O_4 nanoparticles (Red diagram).

All together, these analyses are indicative of the successful immobilization of Cu (0) complex onto the Fe_3O_4@ Schiff-base.

3.3 Catalytic Studies

After the successful characterization of the prepared nanomaterial, the catalytic activities in the synthesis of polyhydroquinoline derivatives were evaluated.

Table 1 Optimization for the synthesis of polyhydroquinolines

Entry[a]	Cat. (mol%)	Solvent	Temp.(°C)	Time. (min)	Yield[b](%)
1	–	H_2O	Reflux	2 day	NR
2	0.05	H_2O	Reflux	15	43
3	0.10	H_2O	Reflux	15	69
4	0.15	H_2O	Reflux	15	83
5	0.20	H_2O	Reflux	15	91
6	0.25	H_2O	Reflux	15	100
7	0.25	Ethanol	Reflux	15	65
8	0.25	PEG-400	100	15	83
9	0.25	DMSO	100	15	52
10	0.25	Dioxane	Reflux	15	70
11	0.25	DMF	100	15	81
12	0.25	Solvent free	100	15	73
13	0.25	H_2O	90	15	89
14	0.25	H_2O	80	15	83
15	0.25	H_2O	60	15	76
16	0.25	H_2O	40	15	64
17	0.25	H_2O	25	15	39

[a] Reaction conditions: 4-chlorobenzaldehyde (1.0 mmol), dimedone (1 mmol), ethyl acetoacetate (1 mmol), and ammonium acetate (1.2 mmol), Catalyst and solvent (2 mL)

[b] Isolated yield

In order to optimize the reaction conditions, the combination of p-Clbenzaldehyde (1 mmol), ethyl acetoacetate (1 mmol), dimedone (1 mmol) and ammonium acetate (1.2 mmol) was chosen as the model reaction to evaluate the optimized catalytic activity. Moreover, the effect of various experimental parameters; including, the effect of diffrent amounts of catalyst, diffrent solvents and the effect of various temperatures on the selected model substrate were screened to achieve high catalytic efficiency and yield. The results are summarized in Table 1. The influence of the catalyst loading on the reaction efficiency was studied with different amounts of the catalyst.The comparison of the results related to the effect of various amounts of the catalyst revealed that the highest activity was observed in the presence of 0.25 mol % of the catalyst on the basis of Cu (Table 1, Entry 6). As can be seen from Table 1, entry 1, the reaction was not completed in the absence of the catalyst even after 2 days. Then, the effects of solvent and reaction temperature were evaluated on the model reaction.

Table 2 Synthesis of polyhydroquinoline derivative

Entry[a]	Aldehyde	Time (min)	Yield (%)[b]	TOF (s^{-1})	M.P	
					Measured	Reported
1	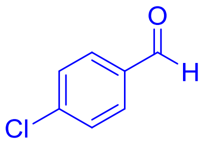	15	100	5,760,000	244–246	243–245 [104]
2	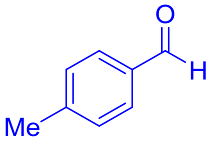	25	96	3,318,290	192–194	252–255 [105]
3	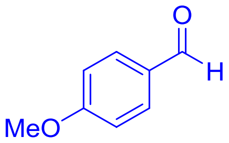	20	98	4,234,023	256–258	251–252 [106]
4	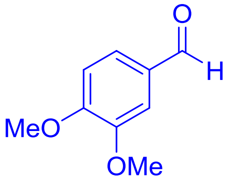	35	92	2,271,215	216–218	216–218 [107]
5	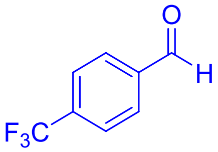	25	91	3,145,463	188–190	188–190 [107]
6	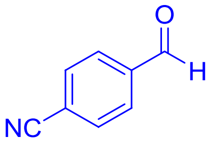	20	95	4,104,410	140–143	140–142 [107]
7	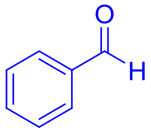	20	99	4,320,000	202–204	203–205 [104]
8	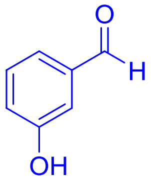	30	93	2,678,400	230–232	231–234 [108]

Table 2 (continued)

Entry[a]	Aldehyde	Time (min)	Yield (%)[b]	TOF (s^{-1})	M.P	
					Measured	Reported
9	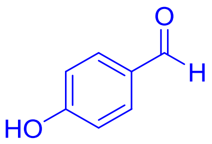	35	95	2,345,276	223–225	225–227 [104]
10	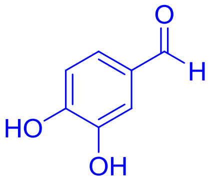	20	92	3,974,797	216–218	216–218 [107]
11	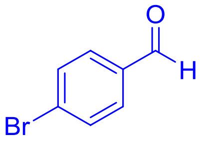	20	97	4,190,819	247–249	249–251 [104]
12	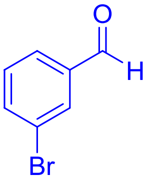	15	91	5,241,600	232–235	231–233 [104]
13	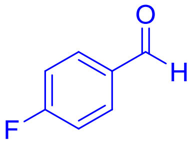	20	95	4,104,410	178–180	180–182 [104]
14	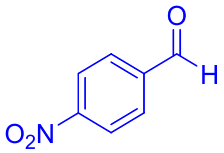	35	94	2,320,589	241–243	241–243 [104]
15	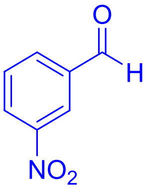	15	92	5,299,200	176–177	176–177 [107]

Table 2 (continued)

Entry[a]	Aldehyde	Time (min)	Yield (%)[b]	TOF (s^{-1})	M.P	
					Measured	Reported
16	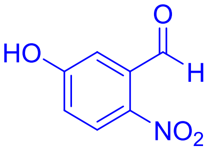	15	90	5,184,000	167–169	167–169 [107]
17	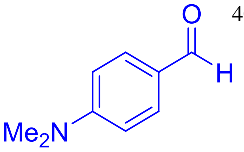	40	94	2,030,603	261–263	261–263 [104]
18	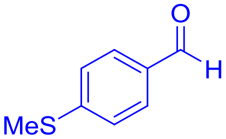	35	93	2,295,902	241–243	240–242 [104]

[a] Reaction conditions: aromatic aldehyde (1.0 mmol), dimedone (1 mmol), ethyl acetoacetate (1 mmol), and ammonium acetate (1.2 mmol), Catalyst (0.25 mol %) and H_2O (3 mL)

[b] Isolated yield

Considering the reaction time and the product yield, H_2O at reflux conditions proved to be the best choice for the solvent and tempereature, respectively. After an extensive screening of the reaction parameters, as shown in Table 1, the best yield of polyhydroquinoline product was obtained specifically when the reaction was performed using 0.25 mol% of Fe_3O_4@Schiff-Base-Cu in H_2O at 100 °C (Table 1, Entry 6).

Then, the catalytic effectiveness of the prepared Fe_3O_4@ Schiff-Base-Cu catalyst was investigated in the synthesis of polyhydroquinoline derivatives via the reaction of different aromatic aldehydes. The results are listed in (Table 2). As shown in Table 2, various aromatic aldehydes bearing different electron-withdrawing group or electron-donating groups, such as OCH_3, NO_2, NMe_2 CH_3, CF_3, SMe, CN, OH, F, Cl, and Br, produced excellent reaction yields in the presence of Fe_3O_4@Schiff-Base-Cu catalyst (Scheme 2).

A plausible mechanism for the multicomponent synthesis of polyhydroquinolines on the basis of previous reports [109] has been depicted in Scheme 3. Based on this mechanism, the role of Fe_3O_4@Schiff-Base-Cu MNPS as a Lewis acid catalyst comes in the Knoevenagel condensation of aldehydes with active methylene compounds (dimedone or ethyl acetoacetate) to produce an α,β-unsaturated compound. In the next step, Fe_3O_4@Schiff-Base-Cu MNPS catalyzed the Michael addition of intermediates to obtain the polyhydroquinoline (Scheme 3).

3.4 Recyclability of the Catalyst

Reproducibility of catalysts provides an important advantage in industrial applications because it reduces production costs. Therefore, the recovery and reproducibility of Fe_3O_4@Schiff-Base-Cu catalyst were explored in the model reaction. After the completion of the experiment, the reaction system was cooled to room temperature and the catalyst was magnetically separated from the solution, washed with acetone, air-dried and, finally, reused for the next round of the reactions. As shown in Fig. 9, the recycling process was repeated for five cycles with a slight decrease in the activity of the catalyst.

Also, in order to examine stability of the catalyst after recycling, the recycled catalyst has been characterized by XRD, SEM, VSM and FT-IR techniques. These characterizations confirmed that the recovered catalyst is in good agreement with the fresh catalyst. These characterizations are strong evidences for high stability of Fe_3O_4@Schiff-base-Cu organometallic complex after recycling.

The SEM image of the recycled catalyst is shown in Fig. 4 (e) in which the morphology of the recovered catalyst is similar to the particle form of the fresh catalyst. Moreover, Fig. 10 shows the XRD pattern of the recovered catalyst and, also, the curve intensity which indicates the structural stability of the catalyst after 11 consecutive cycles.

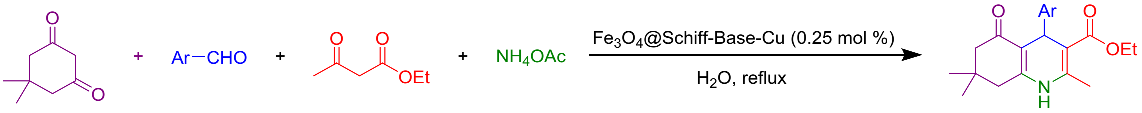

Scheme 2 Fe_3O_4@Schiff-Base-Cu catalyzed the synthesis of polyhydroquinolines

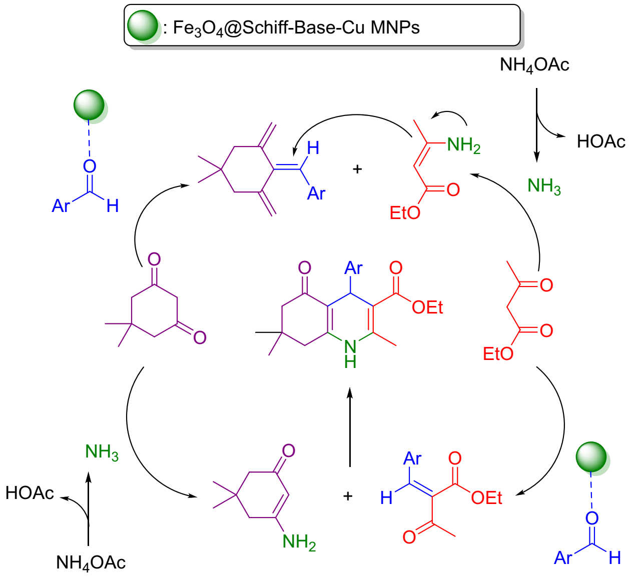

Scheme 3 Proposed mechanism for the synthesis of polyhydroquinolines in the presence of Fe_3O_4@Schiff-Base-Cu catalyst

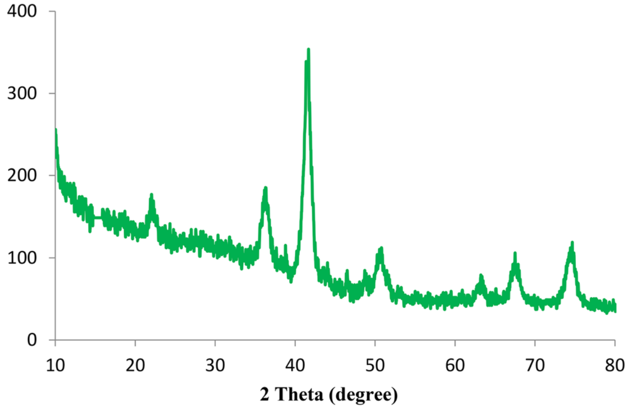

Fig. 10 XRD pattern of the recycled Fe_3O_4@Schiff-Base-Cu

Fig. 9 Reusability of Fe_3O_4@Schiff-Base-Cu

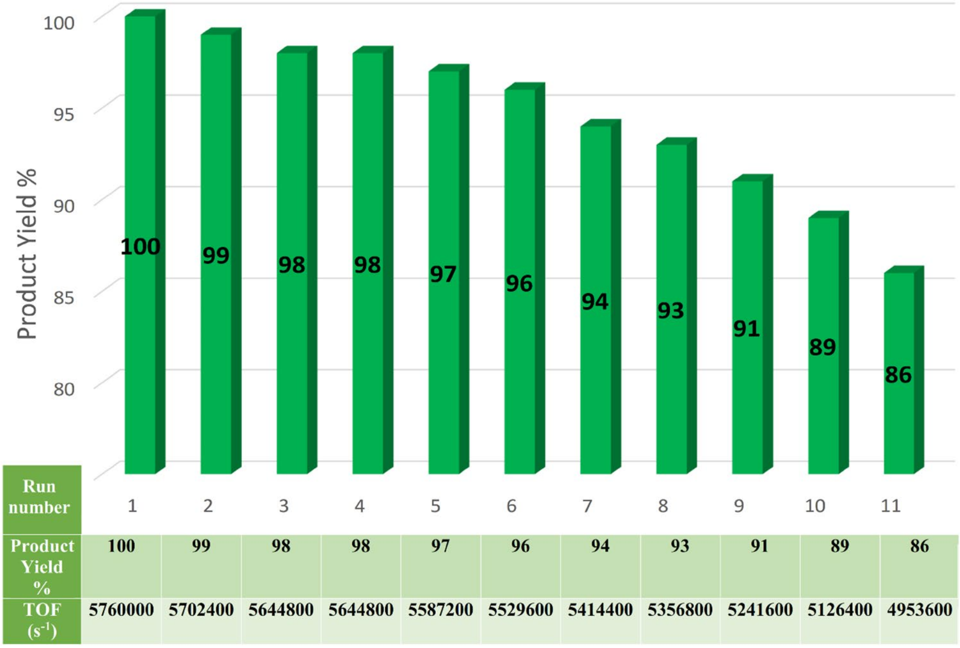

Run number	1	2	3	4	5	6	7	8	9	10	11
Product Yield %	100	99	98	98	97	96	94	93	91	89	86
TOF (s^{-1})	5760000	5702400	5644800	5644800	5587200	5529600	5414400	5356800	5241600	5126400	4953600

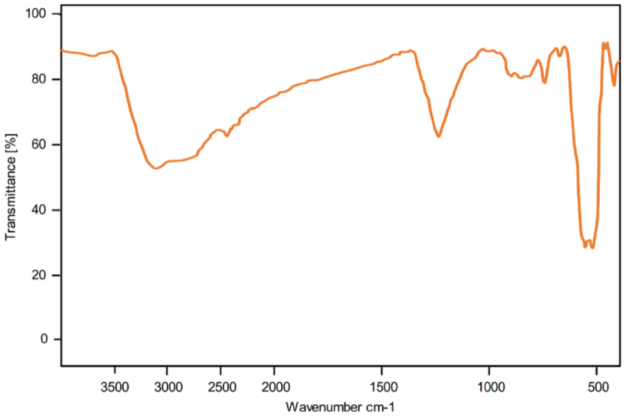

Fig. 11 FT-IR spectra of the recycled Fe_3O_4@Schiff-Base-Cu

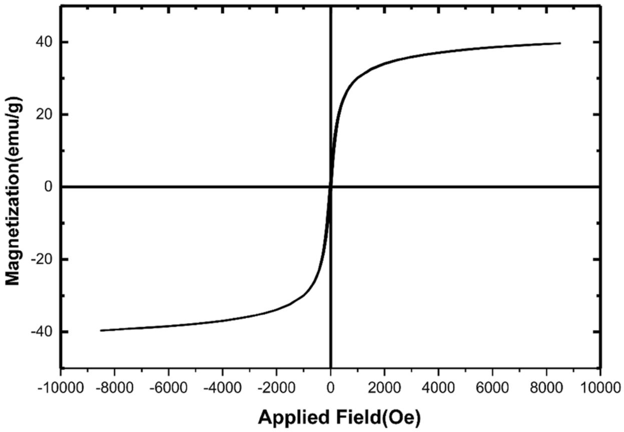

Fig. 12 VSM spectrum of recycled Fe_3O_4@SiO_2-Glycerol-Cu(II)

The Fig. 11 shows the FT-IR spectrum of the recycled Fe_3O_4@Schiff-base-Cu that points out that the catalyst is stable during the organic reactions.

Figure 12 exhibits the magnetization curve of the recycled catalyst. The magnetization curves of the recycled Fe_3O_4@SiO_2-Glycerol-Cu(II) points out that the catalyst is stable during the organic reactions after 11 cycles.

3.5 Leaching Study

In order to consider the leaching of Cu into the reaction media, ICP-AES analysis was performed. In this sense, the copper content in the reaction media and in the model reaction was found to be 0.18%. The results show that the leaching of Cu during the reaction process is negligible and the catalyst is heterogeneous.

3.6 Comparison

In order to investigate the efficiency of this new procedure in comparison to the reported procedures in the literature, the results for the synthesis of polyhydroquinolines using p-Clbenzaldehyde, as the representative example, were compared to the best of the well-known data from the literature outlined in the Table 3. As it is evident from Tables 3, the synthesized Fe_3O_4@Schiff-Base-Cu nanocatalyst showed better results than other methods.

4 Conclusion

In conclusion, the Fe_3O_4@Schiff-Base-Cu catalyst was synthesized and successfully applied for the synthesis of polyhydroquinoline derivatives in water as a green reaction media. The prepared magnetic nanocatalyst was characterized by FT-IR, XRD, EDS, ICP, SEM, X-ray mapping, TGA, and VSM analysis techniques. In addition, all reactions were carried out in green conditions. Additionally, the Fe_3O_4@Schiff-Base-Cu is more economic and environmentally friendly because of its low Cu leaching. This method offers several advantages; including, price, higher catalytic efficiency with lower copper content, heterogeneous nature, wide substrate scope, green conditions, high yield, short reaction time, simple work-up procedure, ease of separation, and recyclability of the magnetic catalyst.

Table 3 Comparison of the Synthesis of polyhydroquinolines in the presence of Fe_3O_4@Schiff-Base-Cu using p-Clbenzaldehyd with previously reported procedure

Entry	Catalyst	Time (min)	Yield (%)[a]	References
1	Fe_3O_4	6	94	[110]
2	$NiFe_2O_4$	3	90	[3]
3	$BiFeO_3$	15	95	[111]
4	$FeAl_2O_4$	180	90	[109]
5	Fe_2O_3@HAp@Melamine	15	93	[112]
6	Cu-SPATBA/Fe_3O_4	65	98	[113]
7	Pd-SBTU@Fe_3O_4	140	95	[114]
8	Fe_3O_4-Adenine-Ni	145	96	[115]
9	γ-Fe_2O_3/Cu@cellulose	15	98	[116]
10	Ru^{III} @CMC/Fe_3O_4	15	95	[117]
11	Fe_3O_4-SA-PPCA	120	95	[118]
12	Fe_3O_4/TiO_2–SO_3H	5	91	[119]
13	GSA@Fe_3O_4	200	94	[120]
14	Fe_3O_4@TDI@TiO_2-SO_3H	10	93	[121]
15	Fe_3O_4/SiO_2-OSO_3H	50	89	[122]
16	Fe_3O_4@PEO-SO_3H	15	94	[123]
17	Fe_3O_4@FSM-16-SO_3H	25	86	[124]
18	Fe_3O_4@D-NH-$(CH_2)_4$-SO_3H	90	86	[125]
19	Fe_3O_4-TEDETA-Br_3	120	92	[126]
20	Fe_3O_4@SiO_2@$(CH_2)_3$Im}$C(NO_2)_3$	18	89	[108]
21	Fe_3O_4@SiO_2@$(CH_2)_3$Im}$C(CN)_3$	20	92	[127]
22	NMSMSA	20	93	[128]
23	AIL-SCMNPs	15	80	[95]
24	BIL@MNP	20	89	[129]
25	Fe_3O_4@SiO_2–PEG/NH_2	20	96	[130]
26	Fe_3O_4@SiO_2@PPh_3@$Cr_2O_7^{2-}$	15	98	[131]
27	Fe_3O_4@GA@IG	45	89	[132]
28	MCM41@Serine@Cu(II)	170	96	[105]
29	SBA-15@Glycine- Ni	110	92	[133]
30	SBA-15@Glycine-Cu	100	94	[133]
31	SBA-15@AMPD-Co	35	97	[106]
32	Nicotinic acid	5	92	[134]
33	Fe_3O_4@Schiff-Base-Cu	15	100	This work

[a] Isolated yield

References

1. Jamale DK, Undare SS, Valekar NJ et al (2019) Glycerol mediated synthesis, biological evaluation, and molecular docking study of 4-(1H-pyrazol-4-yl)-polyhydroquinolines as potent antitubercular agents. J Heterocycl Chem 56:608–618. https://doi.org/10.1002/jhet.3438
2. Saghanezhad SJ, Sayahi MH, Imanifar I et al (2017) Caffeine-H3PO4: a novel acidic catalyst for various one-pot multicomponent reactions. Res Chem Intermed 43:6521–6536
3. Ahankar H, Ramazani A, Joo SW (2016) Magnetic nickel ferrite nanoparticles as an efficient catalyst for the preparation of polyhydroquinoline derivatives under microwave irradiation in solvent-free conditions. Res Chem Intermed 42:2487–2500. https://doi.org/10.1007/s11164-015-2163-6
4. Jadhvar SC, Kasraliker HM, Goswami SV et al (2017) One-pot synthesis and evaluation of anticancer activity of polyhydroquinoline derivatives catalyzed by [Msim]Cl. Res Chem Intermed 43:7211–7221. https://doi.org/10.1007/s11164-017-3069-2
5. Gong G-H, Bian M, Liu C-Y, Zhang B (2019) Heterocyclic pyran and polyhydroquinoline derivatives to inhibit human breast cancer cells. Main Gr Chem 18:15–22. https://doi.org/10.3233/MGC-180676
6. Laughlin TJ, Yoo JS, Mohan RS (2017) Synthesis of 3, 4-dihydropyrimidin-2 (1H)-ones/thiones and polyhydroquinolines via multicomponent reactions. multicomponent reactions. CRC Press, Boca Raton, pp 369–378
7. Amoli T, Baghbanian SM (2018) Poly(vinylimidazolum acetic acid)-entrapped nanozeolite: efficient heterogeneous catalyst for synthesis of polyhydroquinolines and 1,4-dihydropyridines. Res Chem Intermed 44:3389–3405
8. Mohammadi Ziarani G, Seyedakbari L, Asadi S et al (2016) Ionic liquid supported nanoporous silica (SBA-IL) as an efficient and heterogeneous catalyst in the domino synthesis of polyhydroquinoline derivatives. Res Chem Intermed 42:499–509

9. El-Saghier AM, Abd El-Halim HF, Abdel-Rahman LH, Kadry A (2019) Green synthesis of new trizole based heterocyclic amino acids ligands and their transition metal complexes. Characterization, kinetics, antimicrobial and docking studies. Appl Organomet Chem. https://doi.org/10.1002/aoc.4641
10. Zhang G, Liu B, Zhou H et al (2018) Graphene wrapped phthalocyanine: enhanced oxidative desulfurization for dibenzothiophene in fuel. Appl Organomet Chem. https://doi.org/10.1002/aoc.4477
11. Alinezhad H, Mohseni Tavakkoli S (2015) Cu-doped ZnO nanocrystalline powder as a catalyst for green and convenient multi-component synthesis of 1,4-dihydropyridine. Res Chem Intermed 41:5931–5940. https://doi.org/10.1007/s11164-014-1712-8
12. Vahdat SM (2013) Cu(2) schiff base complex as a highly efficient catalyst for the synthesis of polyhydroquinoline derivatives via hantzsch condensation in water. Comb Chem High Throughput Screen 16:782–787. https://doi.org/10.2174/13862073113169990003
13. Taghavi Fardood S, Ramazani A, Golfar Z, Joo SW (2017) Green synthesis of Ni-Cu-Zn ferrite nanoparticles using tragacanth gum and their use as an efficient catalyst for the synthesis of polyhydroquinoline derivatives. Appl Organomet Chem. https://doi.org/10.1002/aoc.3823
14. Tamoradi T, Ghadermazi M, Ghorbani-Choghamarani A (2018) Synthesis of polyhydroquinoline, 2,3-dihydroquinazolin-4(1H)-one, sulfide and sulfoxide derivatives catalyzed by new copper complex supported on MCM-41. Catal Lett 148:857–872. https://doi.org/10.1007/s10562-018-2311-x
15. Ghorbani-Choghamarani A, Tahmasbi B, Moradi P, Havasi N (2016) Cu–S-(propyl)-2-aminobenzothioate on magnetic nanoparticles: highly efficient and reusable catalyst for synthesis of polyhydroquinoline derivatives and oxidation of sulfides. Appl Organomet Chem 30:619–625. https://doi.org/10.1002/aoc.3478
16. Mansoor SS, Aswin K, Logaiya K et al (2014) Silica-supported perchloric acid (HClO4-SiO2): a mild, reusable and highly efficient heterogeneous catalyst for multicomponent synthesis of 1,4-dihydropyridines via unsymmetrical Hantzsch reaction. Res Chem Intermed 40:357–369. https://doi.org/10.1007/s11164-012-0968-0
17. Anbia M, Aghadoukht F (2019) Functionalization of silicon nanowires by iron oxide and copper for degradation of phenol. Res Chem Intermed 45:1973–1984
18. Sayahi MH, Bahadorikhalili S, Saghanezhad SJ, Mahdavi M (2018) Copper (II)-supported polyethylenimine-functionalized magnetic graphene oxide as a catalyst for the green synthesis of 2-arylquinazolin-4(3H)-ones. Res Chem Intermed 44:5241–5253
19. Padmaja RD, Meena DR, Maiti B, Chanda K (2017) [Cu(phen)(PPh3)2]NO3-catalyzed microwave-assisted green synthesis of 5-substituted 1H-tetrazoles. Res Chem Intermed 43:7365–7374
20. Danopoulos AA, Simler T, Braunstein P (2019) N-heterocyclic carbene complexes of copper, nickel, and cobalt. Chem Rev 119:3730–3961. https://doi.org/10.1021/acs.chemrev.8b00505
21. Mandal S, Mandal S, Biswas S et al (2018) Synthesis of 2-(ethynyloxy)naphthaene-1-carbaldehyde using 2-hydroxy benzyl alcohol and propargyl bromide in aqueous micellar media. Res Chem Intermed 44:2169–2177
22. Kobayashi Y, Yasuda Y, Morita T (2016) Recent advances in the synthesis of copper-based nanoparticles for metal–metal bonding processes. J Sci Adv Mater Dev 1:413–430. https://doi.org/10.1016/j.jsamd.2016.11.002
23. Yang Z, Dong A, Chen H (2017) Cu/zeolite catalysts for the photocatalytic decomposition and selective catalytic reduction of NOx. Res Chem Intermed 43:5245–5259
24. Chen L, Noory Fajer A, Yessimbekov Z et al (2019) Diaryl sulfides synthesis: copper catalysts in C-S bond formation. J Sulfur Chem 40:451–468. https://doi.org/10.1080/17415993.2019.1596268
25. Schlichter S, Rocha M, Peixoto AF et al (2018) Copper mesoporous materials as highly efficient recyclable catalysts for the reduction of 4-nitrophenol in aqueous media. Polyhedron 150:69–76. https://doi.org/10.1016/j.poly.2018.04.037
26. Hajipour AR, Fakhari F, Bidhendi GN (2019) Copper nanoparticles supported on 2-methoxy-1-phenylethanone-functionalized MCM-41: an efficient and recyclable catalyst for one-pot three-component C-S coupling reaction of aryl halides with benzyl bromide and thiourea. Appl Organomet Chem. https://doi.org/10.1002/aoc.4853
27. Tamoradi T, Ghorbani-Choghamarani A, Ghadermazi M, Veisi H (2019) SBA-15@Glycine-M (M = Ni and Cu): two green, novel and efficient catalysts for the one-pot synthesis of 5-substituted tetrazole and polyhydroquinoline derivatives. Solid State Sci 91:96–107. https://doi.org/10.1016/j.solidstatesciences.2019.03.020
28. Wang J, Zhou Y, Shao Y et al (2019) Chitosan–silica nanoparticles catalyst (M@CS–SiO 2) for the degradation of 1,1-dimethylhydrazine. Res Chem Intermed 45:1721–1735
29. Fodor A, Hell Z, Pirault-Roy L (2014) Copper(II)- and palladium(II)-modified molecular sieve, a reusable catalyst for the Suzuki-Miyaura-coupling. Appl Catal A 484:39–50. https://doi.org/10.1016/j.apcata.2014.07.002
30. Liu QX, Zhao DX, Wu H et al (2018) Catalytic activities of NHC-PdCl 2 species based on functionalized tetradentate imidazolium salt in three types of C-C coupling reactions. Appl Organomet Chem. https://doi.org/10.1002/aoc.4429
31. Rezvani MA, Aghbolagh ZS, Monfared HH (2018) Green and efficient organic–inorganic hybrid nanocatalyst for oxidative desulfurization of gasoline. Appl Organomet Chem. https://doi.org/10.1002/aoc.4592
32. Hoffmann F, Cornelius M, Morell J, Fröba M (2006) Silica-based mesoporous organic–inorganic hybrid materials. Angew Chem Int Ed 45:3216–3251
33. Aryan R, Beyzaei H, Nojavan M, Dianatipour T (2016) Secondary amines immobilized inside magnetic mesoporous materials as a recyclable basic and oxidative heterogeneous nanocatalyst for the synthesis of trisubstituted pyrimidine derivatives. Res Chem Intermed 42:4417–4431
34. Lashgari N, Badiei A, Ziarani GM (2016) Modification of mesoporous silica SBA-15 with different organic molecules to gain chemical sensors: a review organic molecules and its role. Nano Chem Res 1:127–141. https://doi.org/10.7508/ncr.2016.01.014
35. Liu H, Wei L, Liu F et al (2019) Homogeneous, heterogeneous, and biological catalysts for electrochemical N2 reduction toward NH3 under ambient conditions. ACS Catal. https://doi.org/10.1021/acscatal.9b00994
36. Yin Q, Zhu Y, Ju S et al (2016) Rapid determination of copper and lead in Panax notoginseng by magnetic solid-phase extraction and flame atomic absorption spectrometry. Res Chem Intermed 42:4985–4998
37. Pradhan N, Singh S, Ojha N et al (2015) Facets of nanotechnology as seen in food processing, packaging, and preservation industry. Biomed Res Int. https://doi.org/10.1155/2015/365672
38. Esmaeili-Zare M, Salavati-Niasari M (2015) Synthesis, characterization, and photoluminescence properties of HgSe nanoparticles using a novel mercury precursor by the sonochemical method. Res Chem Intermed 41:8185–8198
39. Jenita Rani G, Jothi Rajan MA, Gnana kumar G (2017) Reduced graphene oxide/ZnFe2O4 nanocomposite as an efficient catalyst for the photocatalytic degradation of methylene blue dye. Res Chem Intermed 43:2669–2690

40. Surynek M, Spanhel L, Lapcik L, Mrazek J (2019) Tuning the photocatalytic properties of sol–gel-derived single, coupled, and alloyed ZnO–TiO2 nanoparticles. Res Chem Intermed. https://doi.org/10.1007/s11164-019-03900-6
41. Zhao Y, Zhao N, Zou M et al (2016) Highly ordered amphiphilic cyclopalladated arylimine self-assembly films for catalyzing Heck and Suzuki coupling reactions. Appl Organomet Chem 30:540–549. https://doi.org/10.1002/aoc.3467
42. Nosrati H, Salehiabar M, Davaran S et al (2017) New advances strategies for surface functionalization of iron oxide magnetic nano particles (IONPs). Res Chem Intermed 43:7423–7442
43. Olad A, Rezvani F, Nosrati R (2018) Preparation and characterization of polyurethane based self-cleaning and antibacterial coating containing silver ion exchanged montmorillonite/TiO2 nanocomposite. Res Chem Intermed 44:1711–1727
44. Razmara Z (2019) Lanthanum(III) complex as ferromagnetic supraprecursor for preparation of La_2O_3 nanoparticles by thermal decomposition method. Res Chem Intermed 45:2887–2901
45. Rostami M, Aghajanzadeh M, Zamani M et al (2018) Sonochemical synthesis and characterization of Fe3O4@mTiO2-GO nanocarriers for dual-targeted colon drug delivery. Res Chem Intermed 44:1889–1904
46. Kiš E, Marinković-Neducin R, Lomić G et al (1998) Structural and textural properties of the NiO-Al2O3 catalyst. Polyhedron 17:27–34. https://doi.org/10.1016/S0277-5387(97)00263-5
47. Ludvíková J, Jabłońska M, Jirátová K et al (2016) Co-Mn-Al mixed oxides as catalysts for ammonia oxidation to N2O. Res Chem Intermed 42:2669–2690
48. Rafiee E, Khodayari M (2016) Starch as a green source for Fe3O4@carbon core-shell nanoparticles synthesis: a support for 12-tungstophosphoric acid, synthesis, characterization, and application as an efficient catalyst. Res Chem Intermed 42:3523–3536
49. Azizi N, Farhadi E (2018) Magnetically separable g-C3N4 hybrid nanocomposite: highly efficient and eco-friendly recyclable catalyst for one-pot synthesis of α-aminonitriles. Appl Organomet Chem. https://doi.org/10.1002/aoc.4188
50. Aghayee M, Zolfigol MA, Keypour H et al (2016) Synthesis and characterization of a novel magnetic nano-palladium Schiff base complex: application in cross-coupling reactions. Appl Organomet Chem 30:612–618. https://doi.org/10.1002/aoc.3477
51. Rakhtshah J, Salehzadeh S, Zolfigol MA, Baghery S (2017) Synthesis, characterization and heterogeneous catalytic application of a nickel(II) Schiff base complex immobilized on MWCNTs for the Hantzsch four-component condensation. J Coord Chem 70:340–360. https://doi.org/10.1080/00958972.2016.1253068
52. Kiyani H, Ghiasi M (2015) Solvent-free efficient one-pot synthesis of Biginelli and Hantzsch compounds catalyzed by potassium phthalimide as a green and reusable organocatalyst. Res Chem Intermed 41:5177–5203. https://doi.org/10.1007/s11164-014-1621-x
53. Zolfigol MA, Bahrami-Nejad N, Baghery S (2016) A convenient method for the synthesis of 1,8-dioxodecahydroacridine derivatives using 1-methylimidazolium tricyanomethanide [HMIM]C(CN)3 as a nanostructured molten salt catalyst. J Mol Liq 218:558–564. https://doi.org/10.1016/j.molliq.2016.03.006
54. Rakhtshah J, Salehzadeh S, Gowdini E et al (2016) Synthesis of pyrazole derivatives in the presence of a dioxomolybdenum complex supported on silica-coated magnetite nanoparticles as an efficient and easily recyclable catalyst. RSC Adv 6:104875–104885. https://doi.org/10.1039/c6ra20988b
55. Atashkar B, Zolfigol MA, Mallakpour S (2018) Applications of biological urea-based catalysts in chemical processes. Mol Catal 452:192–246. https://doi.org/10.1016/j.mcat.2018.03.009
56. Khazaei A, Zolfigol MA, Abedian N (2001) A novel synthesis and characterization of poly[4-imino(n-4-ethylbenzoate)benzene p-styrenesulphonate] and the investigation on polymer ability for drug release. Iran Polym J 10:59–65
57. Lashanizadegan M, Zareian Z (2011) Homogenous and heterogeneous catalytic activity of Azo-linked Schiff base complexes of Mn(II), Cu(II) and Co(II). Catal Lett 141:1698–1702. https://doi.org/10.1007/s10562-011-0709-9
58. Chen L, Li B, Liu D (2014) Schiff base complex coated Fe3O4 nanoparticles: a highly recyclable nanocatalyst for selective oxidation of alkyl aromatics. Catal Lett 144:1053–1061. https://doi.org/10.1007/s10562-014-1244-2
59. Bhoware SS, Kamble KR, Singh AP (2009) Catalytic activity of cobalt containing MCM-41 and HMS in liquid phase oxidation of diphenylmethane. Catal Lett 133:106–111. https://doi.org/10.1007/s10562-009-0162-1
60. Yang D, Gao L, Zhao W (2008) Synthesis, characterization and catalytic activity of dialdehyde starch-schiff base Co(II) complex in the oxidation of cyclohexane. Catal Lett 126:84–88. https://doi.org/10.1007/s10562-008-9579-1
61. Wang X, Qiu Z, Liu Q et al (2017) Heterogeneous catalytic transfer partial-hydrogenation with formic acid as hydrogen source over the schiff-base modified gold nano-catalyst. Catal Lett 147:517–524. https://doi.org/10.1007/s10562-016-1929-9
62. Maruyama K, Tsutsui T, Shiosaki H et al (1993) Structural requirement for catalytic activity of cobalt Schiff base complex in oxygenation of alkenes. React Kinet Catal Lett 49:1–6. https://doi.org/10.1007/BF02084021
63. Haghshenas Kashani S, Moghadam M, Tangestaninejad S et al (2018) Ruthenium nanoparticles immobilized on nano-silica functionalized with thiol-based dendrimer: a nanocomposite material for oxidation of alcohols and epoxidation of alkenes. Catal Lett 148:1110–1123. https://doi.org/10.1007/s10562-018-2313-8
64. Feizpour F, Jafarpour M, Rezaeifard A (2018) A tandem aerobic photocatalytic synthesis of benzimidazoles by cobalt ascorbic acid complex coated on TiO2 nanoparticles under visible light. Catal Lett 148:30–40. https://doi.org/10.1007/s10562-017-2232-0
65. Mirjalili BBF, Soltani R (2019) Nano-kaolin/Ti 4+/Fe 3 O 4: a magnetic reusable nano-catalyst for the synthesis of pyrimido[2,1- b]benzothiazoles. RSC Adv 9:18720–18727. https://doi.org/10.1039/c9ra01767d
66. Hamrahian SA, Rakhtshah J, Mousavi Davijani SM, Salehzadeh S (2018) Copper Schiff base complex immobilized on silica-coated Fe3O4 nanoparticles: a recoverable and efficient catalyst for synthesis of polysubstituted pyrroles. Appl Organomet Chem. https://doi.org/10.1002/aoc.4501
67. Moosavi-Zare AR, Goudarziafshar H, Jalilian Z (2019) Nano-Zn[2-boromophenylsalicylaldiminemethylpyranopyrazole]Cl2 as a novel nanostructured Schiff base complex and catalyst for the synthesis of pyrano[2,3-d]pyrimidinedione derivatives. Appl Organomet Chem. https://doi.org/10.1002/aoc.4584
68. Nikoorazm M, Ghorbani-Choghamarani A, Khanmoradi M (2016) Synthesis and characterization of Ni(II)-Vanillin-Schiff base-MCM-41 composite as an efficient and reusable nanocatalyst for multicomponent reactions. RSC Adv 6:56549–56561. https://doi.org/10.1039/c6ra09371j
69. Karimi F, Zolfigol MA, Yarie M (2019) A novel and reusable ionically tagged nanomagnetic catalyst: application for the preparation of 2-amino-6-(2-oxo-2H-chromen-3-yl)-4-arylnicotinonitriles via vinylogous anomeric based oxidation. Mol Catal. https://doi.org/10.1016/j.mcat.2018.11.009
70. Rakhtshah J, Salehzadeh S, Zolfigol MA, Baghery S (2017) Mn(III)–pentadentate Schiff base complex supported on multi-walled carbon nanotubes as a green, mild and heterogeneous catalyst for the synthesis of tetrahydrobenzo[b]pyrans via

tandem Knoevenagel-Michael cyclocondensation reaction. Appl Organomet Chem. https://doi.org/10.1002/aoc.3690

71. Hami Dindar M, Yaftian MR, Pilehvari M, Rostamnia S (2015) SBA-15 mesoporous materials decorated with organic ligands: use as adsorbents for heavy metal ions. J Iran Chem Soc 12:561–572. https://doi.org/10.1007/s13738-014-0513-8
72. Jahromi EZ, Divsalar A, Saboury AA et al (2016) Palladium complexes: new candidates for anti-cancer drugs. J Iran Chem Soc 13:967–989. https://doi.org/10.1007/s13738-015-0804-8
73. Asadi M, Mohammadi K, Kiyanfar AH (2006) Donor ligand, basal ligand and solvent effects on the equilibrium constants of triphenylphosphinecobalt(III) schiff base complexes with phosphite ligands. J Iran Chem Soc 3:247–252. https://doi.org/10.1007/BF03247215
74. Abou-Melha KS, Faruk H (2008) Bimetallic complexes of schiff base bis-[4-hydroxycuomarin-3-yl]- 1 N,5 N-thiocarbohydrazone as a potentially dibasic pentadentate ligand. Synthesis, spectral, and antimicrobial properties. J Iran Chem Soc 5:122–134. https://doi.org/10.1007/BF03245825
75. Khalil RA, Jalil AH, Abd-Alrazzak AY (2009) Application of a Schiff base derived from sulfanilamide as an acid-base indicator. J Iran Chem Soc 6:345–352. https://doi.org/10.1007/BF03245844
76. Keypour H, Dehghani-Firouzabadi AA, Rezaeivala M, Goudarziafsharc H (2010) Synthesis and characterization of Cd(II) macrocyclic Schiff base complex with two 2-aminoethyl pendant arms. J Iran Chem Soc 7:820–824. https://doi.org/10.1007/BF03246074
77. Rayati S, Shokoohi S, Bohloulbandi E (2016) Mn(II) and VO(IV) Schiff base complexes encapsulated in nanocavities of zeolite-Y: catalytic activity toward oxidation of alkenes and reduction of aldehydes. J Iran Chem Soc 13:1983–1991. https://doi.org/10.1007/s13738-016-0915-x
78. Rajabi F (2010) Cobalt(II) schiff base functionalized mesoporous silica as an efficient and recyclable chemoselective acetalization catalyst. J Iran Chem Soc 7:695–701. https://doi.org/10.1007/BF03246059
79. Naeimi H, Rabiei K, Rezaei M, Meshkani F (2013) Nanocrystalline magnesium oxide as a solid base catalyst promoted one pot synthesis of gem-dichloroaziridine derivatives under thermal conditions. J Iran Chem Soc 10:161–167. https://doi.org/10.1007/s13738-012-0137-9
80. Nikoorazm M, Ghorbani-Choghamarani A, Panahi A et al (2018) Pd(0)-Schiff-base@MCM-41 as high-efficient and reusable catalyst for C-C coupling reactions. J Iran Chem Soc 15:181–189. https://doi.org/10.1007/s13738-017-1222-x
81. Zarnegaryan A, Pahlevanneshan Z, Moghadam M et al (2019) Copper(II) Schiff base complex immobilized on graphene nanosheets: a heterogeneous catalyst for epoxidation of olefins. J Iran Chem Soc 16:747–756. https://doi.org/10.1007/s13738-018-1552-3
82. Sedaghat T, Monajjemzadeh M (2011) Some new organotin(IV) schiff base adducts: synthesis, spectroscopic characterization and thermal studies. J Iran Chem Soc 8:477–483. https://doi.org/10.1007/BF03249081
83. Maruyama K, Nakamura T, Nakamura S et al (1991) Cobalt schiff base complex catalysed solvolytic ring opening of epoxy compounds. React Kinet Catal Lett 45:165–171. https://doi.org/10.1007/BF02070423
84. Yuan X, Shan G, Li L et al (2015) Methyl group modified MCM-41 supported schiff-base cobalt complex and its catalytic performance in cyclohexane oxidation. Catal Lett 145:868–874. https://doi.org/10.1007/s10562-015-1499-2
85. Ghorbani-Choghamarani A, Derakhshan AA, Hajjami M, Rajabi L (2017) Palladium-alumoxane framework as a novel and reusable nanocatalyst for suzuki-miyaura, stille and heck cross coupling reactions. Catal Lett 147:110–127. https://doi.org/10.1007/s10562-016-1904-5
86. Niakan M, Asadi Z (2019) Selective reduction of nitroarenes catalyzed by sustainable and reusable DNA-supported nickel nanoparticles in water at room temperature. Catal Lett. https://doi.org/10.1007/s10562-019-02741-7
87. Mirzaee M, Bahramian B, Shahraki M et al (2018) Molybdenum containing catalysts grafted on functionalized hydrous zirconia nano-particles for epoxidation of alkenes. Catal Lett 148:3003–3017. https://doi.org/10.1007/s10562-018-2521-2
88. Bondarenko GN, Dvurechenskaya EG, Magommedov ES, Beletskaya IP (2017) Copper(0) nanoparticles supported on Al2O3 as catalyst for carboxylation of terminal alkynes. Catal Lett 147:2570–2580. https://doi.org/10.1007/s10562-017-2127-0
89. Liu M-Q, Weng X-Y, Wang Q et al (2017) Recombinant thermostable thermomonospora fusca TF endo-xylanase A and its immobilization on modified mesoporous SiO2 microspheres for manufacturing xylooligosaccharides. Catal Lett 147:765–772. https://doi.org/10.1007/s10562-017-1979-7
90. Xu X, Liu P, Li S-H et al (2006) Chitosan-supported imine palladacycle complex and its catalytic performance for heck reaction. React Kinet Catal Lett 88:217–223. https://doi.org/10.1007/s11144-006-0055-x
91. Veisi H, Azadbakht R, Saeidifar F, Abdi MR (2017) Schiff base-functionalized multi walled carbon nano tubes to immobilization of palladium nanoparticles as heterogeneous and recyclable nanocatalyst for suzuki reaction in aqueous media under mild conditions. Catal Letters 147:976–986. https://doi.org/10.1007/s10562-016-1963-7
92. Nikoorazm M, Ghorbani F, Ghorbani-Choghamarani A, Erfani Z (2018) Pd(0)- S-propyl-2-aminobenzothioate immobilized onto functionalized magnetic nanoporous MCM-41 as efficient and recyclable nanocatalyst for the Suzuki, Stille and Heck cross coupling reactions. Appl Organomet Chem 32:1–13. https://doi.org/10.1002/aoc.4282
93. Azarkamanzad Z, Farzaneh F, Maghami M et al (2018) Synthesis, characterization and immobilization of a novel mononuclear vanadium (V) complex on modified magnetic nanoparticles as catalyst for epoxidation of allyl alcohols. Appl Organomet Chem. https://doi.org/10.1002/aoc.4168
94. Ma M, Yang Y, Liao D et al (2019) Synthesis, characterization and catalytic performance of core-shell structure magnetic Fe3O4/P(GMA-EGDMA)-NH2/HPG-COOH-Pd catalyst. Appl Organomet Chem 33:e4708. https://doi.org/10.1002/aoc.4708
95. Taheri N, Heidarizadeh F, Kiasat A (2017) A new magnetically recoverable catalyst promoting the synthesis of 1,4-dihydropyridine and polyhydroquinoline derivatives via the Hantzsch condensation under solvent-free conditions. J Magn Magn Mater 428:481–487. https://doi.org/10.1016/j.jmmm.2016.09.099
96. Sarkheil M, Lashanizadegan M (2018) New magnetic supported hydrazone Schiff base dioxomolybdenum (VI) complex: an efficient nanocatalyst for epoxidation of cyclooctene and norbornene. Appl Organomet Chem. https://doi.org/10.1002/aoc.4459
97. Karami K, Jamshidian N, Nikazma MM et al (2018) Hiyama cross-coupling reaction using Pd(II) nanocatalyst immobilized on the surface of Fe3O4@SiO2. Appl Organomet Chem. https://doi.org/10.1002/aoc.3978
98. Sharbatdaran M, Farzaneh F, Larijani MM et al (2016) Synthesis, characterization, DFT studies, and immobilization of cobalt(II) complex with N, N′, N″ -tris(2-pyrimidinyl)dimethylentriamine on modified iron oxide as oxidation catalyst. Polyhedron 115:264–275. https://doi.org/10.1016/j.poly.2016.05.023
99. Nikoorazm M, Ghorbani F, Ghorbani-Choghamarani A, Erfani Z (2018) Nickel Schiff base complex anchored on Fe3O4@MCM-41 as a novel and reusable magnetic nanocatalyst and its

application in the oxidation of sulfides and oxidative coupling of thiols using H_2O_2. Phosphorus Sulfur Silicon Relat Elem 193:552–561. https://doi.org/10.1080/10426507.2018.1455200

100. Veisi H, Rashtiani A, Rostami A et al (2019) Chemo-selective oxidation of sulfide to sulfoxides with H2O2 catalyzed by oxo-vanadium/Schiff-base complex immobilized on modified magnetic Fe3O4 nanoparticles as a heterogeneous and recyclable nanocatalyst. Polyhedron 157:358–366. https://doi.org/10.1016/j.poly.2018.09.034
101. Ghorbani-Choghamarani A, Mohammadi M, Hudson RHE, Tamoradi T (2019) Boehmite@tryptophan-Pd nanoparticles: a new catalyst for C-C bond formation. Appl Organomet Chem 33:e4977. https://doi.org/10.1002/aoc.4977
102. Mirzaee M, Bahramian B, Gholampour P et al (2019) Preparation and characterization of Fe_3O_4 @Boehmite core-shell nanoparticles to support molybdenum or vanadium complexes for catalytic epoxidation of alkenes. Appl Organomet Chem 33:e4792. https://doi.org/10.1002/aoc.4792
103. Ghorbani-Choghamarani A, Rabiei H, Tahmasbi B et al (2016) Preparation of DSA@MNPs and application as heterogeneous and recyclable nanocatalyst for oxidation of sulfides and oxidative coupling of thiols. Res Chem Intermed 42:5723–5737
104. Mohammadi K, Shirini F, Yahyazadeh A (2016) 1, 3-Disulfonic acid imidazolium hydrogen sulphate as an efficient and reusable ionic liquid for the multicomponent synthesis of polyhydroquinoline derivatives under solvent-free conditions. Res Chem Intermed 42:2047–2054. https://doi.org/10.1007/s11164-015-2134-y
105. Tamoradi T, Ghadermazi M, Ghorbani-Choghamarani A (2018) Synthesis of polyhydroquinoline, 2,3-dihydroquinazolin-4(1H)-one, sulfide and sulfoxide derivatives catalyzed by new copper complex supported on MCM-41. Catal Letters 148:857–872. https://doi.org/10.1007/s10562-018-2311-x
106. Ghorbani-Choghamarani A, Mohammadi M, Tamoradi T, Ghadermazi M (2019) Covalent immobilization of Co complex on the surface of SBA-15: green, novel and efficient catalyst for the oxidation of sulfides and synthesis of polyhydroquinoline derivatives in green condition. Polyhedron 158:25–35. https://doi.org/10.1016/j.poly.2018.10.054
107. Surasani R, Kalita D, Rao AVD et al (2012) FeF 3 as a novel catalyst for the synthesis of polyhydroquinoline derivatives via unsymmetrical Hantzsch reaction. J Fluor Chem 135:91–96. https://doi.org/10.1016/j.jfluchem.2011.09.005
108. Yarie M, Zolfigol MA, Bayat Y et al (2016) Novel magnetic nanoparticles with ionic liquid tags as a reusable catalyst in the synthesis of polyhydroquinolines. RSC Adv 6:82842–82853. https://doi.org/10.1039/c6ra16459e
109. Ghorbani-Choghamarani A, Mohammadi M, Shiri L, Taherinia Z (2019) Synthesis and characterization of spinel FeAl2O4 (hercynite) magnetic nanoparticles and their application in multicomponent reactions. Res Chem Intermed (Article inpress). https://doi.org/10.1007/s11164-019-03930-0
110. Nasr-Esfahani M, Hoseini SJ, Montazerozohori M et al (2014) Magnetic Fe3O4 nanoparticles: efficient and recoverable nanocatalyst for the synthesis of polyhydroquinolines and Hantzsch 1,4-dihydropyridines under solvent-free conditions. J Mol Catal A 382:99–105. https://doi.org/10.1016/j.molcata.2013.11.010
111. Khashi M, Allameh S, Beyramabadi SA et al (2017) BiFeo3 magnetic nanoparticles: a novel, efficient and reusable magnetic catalyst for the synthesis of polyhydroquinoline derivatives. Iran J Chem Chem Eng 36:45–52
112. Igder S, Kiasat AR, Shushizadeh MR (2015) Melamine supported on hydroxyapatite-encapsulated-γ-Fe_2O_3: a novel superparamagnetic recyclable basic nanocatalyst for the synthesis of 1,4-dihydropyridines and polyhydroquinolines. Res Chem Intermed 41:7227–7244. https://doi.org/10.1007/s11164-014-1808-1
113. Ghorbani-Choghamarani A, Tahmasbi B, Moradi P, Havasi N (2016) Cu- S -(propyl)-2-aminobenzothioate on magnetic nanoparticles: highly efficient and reusable catalyst for synthesis of polyhydroquinoline derivatives and oxidation of sulfides. Appl Organomet Chem 30:619–625. https://doi.org/10.1002/aoc.3478
114. Ghorbani-Choghamarani A, Tahmasbi B, Moradi Z (2017) S-Benzylisothiourea complex of palladium on magnetic nanoparticles: a highly efficient and reusable nanocatalyst for synthesis of polyhydroquinolines and Suzuki reaction. Appl Organomet Chem 31:e3665. https://doi.org/10.1002/aoc.3665
115. Tamoradi T, Ghadermazi M, Ghorbani-Choghamarani A (2018) Ni(II)-Adenine complex coated Fe 3 O 4 nanoparticles as high reusable nanocatalyst for the synthesis of polyhydroquinoline derivatives and oxidation reactions. Appl Organomet Chem 32:e3974. https://doi.org/10.1002/aoc.3974
116. Maleki A, Eskandarpour V, Rahimi J, Hamidi N (2019) Cellulose matrix embedded copper decorated magnetic bionanocomposite as a green catalyst in the synthesis of dihydropyridines and polyhydroquinolines. Carbohydr Polym 208:251–260. https://doi.org/10.1016/j.carbpol.2018.12.069
117. Chen Y, Zhang Z, Jiang W et al (2019) RuIII@CMC/Fe3O4 hybrid: an efficient, magnetic, retrievable, self-organized nanocatalyst for green synthesis of pyranopyrazole and polyhydroquinoline derivatives. Mol Divers 23:421–442. https://doi.org/10.1007/s11030-018-9887-3
118. Ghorbani-Choghamarani A, Azadi G (2015) Synthesis, characterization, and application of Fe3O4-SA-PPCA as a novel nanomagnetic reusable catalyst for the efficient synthesis of 2,3-dihydroquinazolin-4(1H)-ones and polyhydroquinolines. RSC Adv 5:9752–9758. https://doi.org/10.1039/c4ra15315d
119. Amoozadeh A, Golian S, Rahmani S (2015) TiO2-coated magnetite nanoparticle-supported sulfonic acid as a new, efficient, magnetically separable and reusable heterogeneous solid acid catalyst for multicomponent reactions. RSC Adv 5:45974–45982. https://doi.org/10.1039/c5ra06515a
120. Hajjami M, Tahmasbi B (2015) Synthesis and characterization of glucosulfonic acid supported on Fe 3 O 4 nanoparticles as a novel and magnetically recoverable nanocatalyst and its application in the synthesis of polyhydroquinoline and 2,3-dihydroquinazolin-4(1H)-one derivatives. RSC Adv 5:59194–59203. https://doi.org/10.1039/c5ra08952b
121. Tabrizian E, Amoozadeh A (2016) A new type of SO3H-functionalized magnetic-titania as a robust magnetically-recoverable solid acid nanocatalyst for multi-component reactions. RSC Adv 6:96606–96615. https://doi.org/10.1039/c6ra21048a
122. Maleki A, Akbarzade AR, Bhat AR (2017) Green synthesis of polyhydroquinolines via MCR using Fe3O4/SiO2-OSO3H nanostructure catalyst and prediction of their pharmacological and biological activities by PASS. J Nanostruct Chem 7:309–316. https://doi.org/10.1007/s40097-017-0240-7
123. Azizi M, Maleki A, Hakimpoor F et al (2018) Green Approach for Highly Efficient Synthesis of Polyhydroquinolines Using Fe3O4@PEO-SO3H as a Novel and Recoverable Magnetic Nanocomposite Catalyst. Lett Org Chem 15:753–759
124. Hashemi-Uderji S, Abdollahi-Alibeik M, Ranjbar-Karimi R (2019) Fe_3O_4@FSM-16-SO 3 H as a novel magnetically recoverable nanostructured catalyst: preparation, characterization and catalytic application. J Porous Mater 26:467–480. https://doi.org/10.1007/s10934-018-0628-x
125. Alinezhad H, Tarahomi M, Maleki B, Amiri A (2019) SO 3 H-functionalized nano-MGO-D-NH 2: synthesis, characterization and application for one-pot synthesis of pyrano[2,3-d]pyrimidinone and tetrahydrobenzo[b]pyran derivatives in

aqueous media. Appl Organomet Chem. https://doi.org/10.1002/aoc.4661

126. Hajjami M, Gholamian F (2016) Tribromide ion immobilized on magnetic nanoparticle as a new, efficient and reusable nanocatalyst in multicomponent reactions. RSC Adv 6:87950–87960. https://doi.org/10.1039/c6ra15474c
127. Zolfigol MA, Yarie M (2015) Synthesis and characterization of novel silica-coated magnetic nanoparticles with tags of ionic liquid. Application in the synthesis of polyhydroquinolines. RSC Adv 5:103617–103624. https://doi.org/10.1039/C5RA23670C
128. Zolfigol MA, Ghaderi H, Baghery S, Mohammadi L (2017) Nanometasilica disulfuric acid (NMSDSA) and nanometasilica monosulfuric acid sodium salt (NMSMSA) as two novel nanostructured catalysts: applications in the synthesis of Biginelli-type, polyhydroquinoline and 2,3-dihydroquinazolin-4(1H)-one derivatives. J Iran Chem Soc 14:121–134. https://doi.org/10.1007/s13738-016-0964-1
129. Zhang Q, Ma XM, Wei HX et al (2017) Covalently anchored tertiary amine functionalized ionic liquid on silica coated nano-Fe 3 O 4 as a novel, efficient and magnetically recoverable catalyst for the unsymmetrical Hantzsch reaction and Knoevenagel condensation. RSC Adv 7:53861–53870. https://doi.org/10.1039/c7ra10692k
130. Kardooni R, Kiasat AR, Motamedi H (2017) Designing of a novel dual-function silica-iron oxide hybrid based nanocomposite, Fe3O4@SiO2[sbnd]PEG/NH2, and its application as an eco-catalyst for the solvent-free synthesis of polyhydroacridines and polyhydroquinolines. J Taiwan Inst Chem Eng 81:373–382. https://doi.org/10.1016/j.jtice.2017.10.013
131. Maleki A, Hamidi N, Maleki S, Rahimi J (2018) Surface modified SPIONs-Cr(VI) ions-immobilized organic-inorganic hybrid as a magnetically recyclable nanocatalyst for rapid synthesis of polyhydroquinolines under solvent-free conditions at room temperature. Appl Organomet Chem 32:e4245. https://doi.org/10.1002/aoc.4245
132. Pourian E, Javanshir S, Dolatkhah Z et al (2018) Ultrasonic-Assisted Preparation, Characterization, and Use of Novel Biocompatible Core/Shell Fe 3 O 4 @GA@Isinglass in the Synthesis of 1,4-Dihydropyridine and 4 H -Pyran Derivatives. ACS Omega 3:5012–5020. https://doi.org/10.1021/acsomega.8b00379
133. Tamoradi T, Ghorbani-Choghamarani A, Ghadermazi M, Veisi H (2019) SBA-15@Glycine-M (M = Ni and Cu): two green, novel and efficient catalysts for the one-pot synthesis of 5-substituted tetrazole and polyhydroquinoline derivatives. Solid State Sci 91:96–107. https://doi.org/10.1016/j.solidstatesciences.2019.03.020
134. Davarpanah J, Ghahremani M, Najafi O (2019) Synthesis of 1,4-dihydropyridine and polyhydroquinoline derivatives via Hantzsch reaction using nicotinic acid as a green and reusable catalyst. J Mol Struct 1177:525–535. https://doi.org/10.1016/j.molstruc.2018.10.002

Affiliations

Muhammad Aqeel Ashraf[1,2] · Zhenling Liu[3] · Wan-Xi Peng[1] · Caixia Gao[4]

[1] School of Forestry, Henan Agricultural University, Zhengzhou 450002, China

[2] Department of Geology Faculty of Science, University of Malaya, 50603 Kuala Lumpur, Malaysia

[3] School of Management, Henan University of Technology, Zhengzhou 450001, China

[4] College of Geology and Surveying Engineering, Chongqing Vocationan Institute of Engineering, Chongqing 402260, China